

1 **Title**

2 Pangenomic analysis of *Helcococcus ovis* reveals widespread tetracycline resistance and a novel bacterial
3 species, *Helcococcus bovis*.

4 **Authors**

5 Federico Cunha^{1,*}, Yuting Zhai^{2,3}, Segundo Casaro¹, Kristi L. Jones¹, Modesto Hernandez¹, Rafael S.
6 Bisinotto¹, Subhashinie Kariyawasam⁵, Mary B. Brown^{4,6}, Ashley Phillips⁷, Kwangcheol C. Jeong^{2,3}, Klbs N.
7 Galvão ^{1,4,*}

8 **Affiliations**

9 1. Department of Large Animal Clinical Sciences, University of Florida College of Veterinary Medicine,
10 Gainesville, Florida.

11 2. Department of Animal Sciences, University of Florida College of Agriculture and Life Sciences,
12 Gainesville, Florida.

13 3. Emerging Pathogens Institute, University of Florida, Gainesville, Florida

14 4. D. H. Barron Reproductive and Perinatal Biology Research Program, University of Florida, Gainesville
15 Florida.

16 5. Department of Comparative, Diagnostic, and Population Medicine, University of Florida College of
17 Veterinary Medicine, Gainesville, Florida.

18 6. Department of Infectious Diseases and Immunology, University of Florida College of Veterinary
19 Medicine, Gainesville, Florida.

20 7. Athens Veterinary Diagnostic Laboratory, College of Veterinary Medicine, The University of Georgia,
21 United States.

22

23 * Corresponding authors: fcunha@ufl.edu; galvaok@ufl.edu

24

25 **Abstract**

26 *Helcococcus ovis* (*H. ovis*) is an opportunistic bacterial pathogen of a wide range of animal hosts
27 including domestic ruminants, swine, avians, and humans. In this study, we sequenced the genomes of
28 35 *Helcococcus* sp. clinical isolates from the uterus of dairy cows and explored their antimicrobial
29 resistance and biochemical phenotypes. Phylogenetic and average nucleotide identity analyses placed
30 four *Helcococcus* isolates within a cryptic clade-representing an undescribed species, for which we
31 propose the name *Helcococcus bovis* sp. nov. We applied whole genome comparative analyses to
32 explore the pangenome, resistome, virulome, and taxonomic diversity of the remaining 31 *H. ovis*
33 isolates. *H. ovis* was more often isolated from cows with metritis, however, there was no associations
34 between *H. ovis* gene clusters and uterine infection. The phylogenetic distribution of high-virulence
35 determinants of *H. ovis* is consistent with convergent gene loss in the species. The majority of *H. ovis*
36 strains (30/31) contain mobile tetracycline resistance genes, leading to higher minimum inhibitory
37 concentrations of tetracyclines in vitro. In summary, this study showed that the presence of *H. ovis* is
38 associated with uterine infection in dairy cows, that mobile genetic element-mediated tetracycline
39 resistance is widespread in *H. ovis*, and that there is evidence of co-occurring virulence factors across
40 clades suggesting convergent gene loss in the species. Finally, we introduced a novel *Helcococcus*
41 species closely related to *H. ovis*, called *H. bovis* sp. nov.

42

43 **Highlights**

44 . The presence of *Helcococcus ovis* is associated with uterine infection in dairy cows
45 . Mobile genetic element-mediated tetracycline resistance is widespread in *H. ovis*
46 . Co-occurring virulence factors across clades suggest convergent gene loss in the species
47 . *Helcococcus bovis* is a novel species closely related to *Helcococcus ovis*

48

49 **Introduction**

50 *Helcococcus ovis* (*H. ovis*) belongs to a clinically important genus of bacteria populated by five other
51 described species: *Helcococcus kunzii*, *Helcococcus massiliensis*, *Helcococcus sueciensis*, *Helcococcus*
52 *seattlensis*, and *Helcococcus pyogenes*, all of which are opportunistic pathogens of humans (1–4). Unlike
53 the remaining members of the genus, *H. ovis* is most often found as a co-infecting pathogen in mixed
54 infections of farm animals, such as metritis (5), mastitis (6), and pneumonia (7). Due to these
55 characteristics, its ability to independently cause disease had not been documented until recently (7–
56 10). *H. ovis* is capable of independently causing bovine valvular endocarditis (11), pneumonia, and
57 bursitis (12) in clinical infections, and mastitis in an experimentally infected mouse (*Mus musculus*)
58 model (6). The only confirmed human infection by *H. ovis* originates from a 2018 case study of an
59 artificial eye infection caused by the then-named Tongji strain, which displayed an atypical biochemical
60 profile for the species (13).

61 Although there is abundant data showing the geographical distribution, host range, and
62 infection sites of this pathogen, the mechanisms that lead to the establishment and progression of *H.*
63 *ovis* infections remain unexplored. As shown in an invertebrate infection model, *H. ovis* strains
64 originating from the uterus of dairy cows can display varying degrees of virulence (14). Based on the
65 virulence phenotypes from that study, whole genome comparative analyses identified potential high
66 virulence determinants in this organism, including Zinc ABC transporters, two hypothetical proteins, and
67 a pathogenicity island (15). These comparative analyses created a blueprint for investigating *H. ovis*
68 pathogenic capabilities, but the role these virulence factors may play in disease pathogenesis remains
69 unexplored.

70 One of the most prevalent and costly animal diseases associated with *H. ovis* is metritis in dairy
71 cows (5,16). This disease is characterized by acute uncontrolled opportunistic bacterial proliferation

72 within the uterus in the face of immune dysregulation, leading to painful inflammation, impaired
73 fertility, and sometimes death. The primary causative agents of metritis have not been clearly identified,
74 but studies have shown that *Bacteroides pyogenes*, *Fusobacterium necrophorum*, *Porphyromonas levii*,
75 and *Helcococcus ovis* are of importance in its etiology (5,17,18). Among these organisms, *H. ovis* is
76 atypical in that it is a Gram-positive facultative anaerobic bacterium within an infection environment
77 dominated by Gram-negative obligate anaerobes. Exploring the genomic features and diversity of this
78 bacterium is a key step in unraveling its role in the pathogenesis of mixed infections.

79 Pangenomic analyses can provide valuable insights into the genomic diversity, virulence factors,
80 and potential antimicrobial resistance profiles of bacterial populations. By examining the pangenome,
81 which includes the core genome shared by all isolates and the accessory genome comprising genes
82 unique to specific isolates, we can identify genetic variations that may be associated with virulence or
83 adaptations to the uterine microenvironment in health or disease. A pangenomic analysis of *H. ovis*
84 isolates from the uterus of healthy dairy cows and those with metritis can offer a comprehensive view of
85 the bacterium's genomic characteristics and shed light on its pathogenic potential, host adaptation, and
86 implications for antimicrobial treatment options.

87 In this study, we sequenced the genomes of 35 *Helcococcus* clinical isolates from the uterus of
88 dairy cows and tested their antimicrobial resistance and biochemical phenotypes. Phylogenetic and
89 average nucleotide identity analyses placed 4 *Helcococcus* isolates within a cryptic clade, representing
90 an undescribed species. We applied whole genome comparative analyses to explore the pangenome,
91 resistome, virulome, and taxonomic diversity of the remaining 31 *H. ovis* isolates.

92

93 **Results**

94 ***Helcococcus ovis* Isolation is Associated with Metritis**

95 Of the thirty-eight cows evaluated for metritis diagnosis, twenty-one were healthy and seventeen were
96 diagnosed with metritis. As shown in Table 1, six healthy cows and fifteen cows with metritis were
97 culture-positive for *H. ovis*. We used Fisher's exact test to examine the relationship between metritis
98 and the presence of live *H. ovis* in the uterus, which showed a statistically significant association ($p <$
99 0.001). The odds ratio (OR) for cows with metritis was found to be 18.75 (95% confidence interval: 3.14-
100 92.85), indicating an 18-fold increased risk of being culture-positive for *H. ovis* compared to healthy
101 cows. Clinical data for the cows used for this study and for those associated with strains included from
102 previous studies is presented in Supplemental File 1.

103 **Table 1.** Two-by-two contingency table of *H. ovis* isolation in healthy cows and cows with metritis.

	Healthy	Metritis	Row Sum
<i>H. ovis</i> Positive	6	15	21
<i>H. ovis</i> Negative	15	2	17
Column Sum	21	17	

104 $p < 0.001$, OR=18.75 (95% CI: 3.14-92.85)

105

106 **Read Quality and Assemblies**

107 A total of 30 *H. ovis* isolates were selected for Illumina sequencing. These included 20 recovered from
108 the screening portion of this study and ten previously isolated strains. Illumina reads from two
109 additional *H. ovis* strains (KG39 and KG40) were retrieved from the GenBank to make a total of 32 sets
110 of Illumina reads. Two isolates (KG111 and KG115) were excluded from further analysis because they did
111 not reach the desired coverage threshold of at least 15x. The remaining 30 samples had a mean of 163
112 mega base pairs (Mbp), ranging from 30 to 567. Using an expected *H. ovis* genome size of 1.8Mbp
113 resulted in a mean coverage of 90x, ranging from 16x to 308x. Detailed read quality metrics and SRA
114 accession numbers are listed in Supplemental File 2.

115 Of the resulting de-novo assemblies, five (KG101, KG116, KG93, KG118, KG97) resulted in unexpectedly
116 small genome sizes ranging from 1.02 to 1.48 Mbp compared to the expected range of 1.7-.1.85 Mbp.

117 These genome assemblies also have fewer than the expected >1600 coding sequences (CDS) (1234-
118 1537) and fewer than the expected 33 tRNAs (23-29) found in *H. ovis*, and therefore they were excluded
119 from the pangenome analysis. However, they were retained for other analyses since they can provide
120 valuable taxonomic and gene presence information. Finally, we also included five complete *H. ovis*
121 genomes (KG36, KG37, KG38, KG104, and KG106) from a previous study (15). Genome assembly
122 statistics for all thirty-five genomes included in this study and their accession numbers are listed in
123 Supplemental File 3.

124

125 ***Helcoccoccus* Cryptic Strains**

126 In a recent study we identified a single putative *H. ovis* strain (KG38) whose average nucleotide identity
127 (ANI) with other *H. ovis* strains is lower than the suggested 96% threshold for same species
128 determination (15). Although the initial identification of *H. ovis* isolates for this experiment was
129 conducted based on 16S rRNA sequence identity comparisons, 16S rRNA sequence variations are often
130 not specific enough to discriminate between closely related species (19). To screen for the presence of
131 any cryptic species among our assembled genomes, we created a maximum likelihood phylogenetic tree
132 and evaluated all-vs-all ANI relationships between all the strains in this study.

133

134 *Taxonomy and ANI*

135 As shown in Figure 1, four (KG38, KG95, KG105, and KG197) of the 35 strains included in this study
136 cluster together in a clade forming an outgroup from the remaining 31 *H. ovis* strains. These strains have
137 ANIs lower than 90% with the rest of the *H. ovis* species and also a higher than 96% ANI between each
138 other. Although these three cryptic strains are closely related to *H. ovis*, their taxonomic position within
139 the genus *Helcoccoccus* and family *Peptoniphilaceae* is unclear. We selected one representative *H. ovis*
140 strain for each subclade within the species taxon and created a maximum likelihood phylogenetic tree

141 which also includes the type strains for all species of the *Helcococcus* genus as well as the type species
142 for the most closely related genera to *Helcococcus*: *Finegoldia* and *Parvimonas*. Figure 2 shows this
143 phylogenetic tree alongside a heat map of ANI values between *H. ovis* strains and type strains of other
144 close species and genera. Strains KG38, KG95, KG105, and KG197 form a cryptic clade within
145 *Helcococcus*. Having less than 95% ANI with every other species of the *Helcococcus* genus is evidence
146 that these strains represent a distinct novel species. Furthermore, having a higher than 70% ANI with
147 the type strains of other *Helcococcus* species and less than 70% ANI with *Finegoldia magna* and
148 *Parvimonas micra* is robust evidence that these strains belong to the genus *Helcococcus*. These
149 observations are also supported by the maximum likelihood phylogenetic tree that was constructed with
150 232 orthologous genes shared across stains.

151 Although the only publicly available whole genome sequences of *H. ovis* are from isolates
152 associated with metritis in Holstein dairy cows, there are few publicly available near-complete *H. ovis*
153 16S rRNA sequences. As shown in Figure 3A, a multiple sequence alignment of near-complete *H. ovis*
154 16S rRNA sequences from this study, the Tongji strain, and the *H. ovis* type strain is able to discriminate
155 between the core *H. ovis* clade and the cryptic strains. However, as shown in Figure 3A, these
156 differences are driven by single nucleotide polymorphisms in hypervariable regions V2 and, to a lesser
157 extent, V6. Based on this multiple sequence alignment, the *H. ovis* Tongji strain can also be considered a
158 member of the cryptic *Helcococcus* sp. clade.

159 In an attempt to identify a single marker gene to resolve the two *Helcococcus* sp. groups we also
160 extracted the *rpoB* gene from the same genome assemblies in this study. Although there are no publicly
161 available *rpoB* sequences for *H. ovis*, it is an often-used core gene for bacterial phylogenetic analyses. As
162 shown in Figure 3B, the multiple sequence alignment is able to discriminate between the core *H. ovis*
163 clade and the cryptic strains while also having areas of sequence entropy across the gene, making it a
164 better candidate single marker gene than 16S rRNA for *Helcococcus* species differentiation.

165

166 *Proteome comparison*

167 Finally, as shown in Figure 4, a protein blast alignment between the complete proteomes of three
168 representative *H. ovis* strains (KG36, KG37, and KG106) and three of the cryptic strains (KG38, KG95, and
169 KG105) illustrates that the cryptic strains have protein sequence identities with the reference *H. ovis*
170 KG36 as low as 80-70% across their genomes.

171

172 *Phenotypic characteristics*

173 Phenotypically, the cryptic *Helcococcus* sp. strains are Gram-positive facultative anaerobic cocci that
174 depend on pyridoxine supplementation for growth in vitro. They can be cultivated at 36-38 °C on
175 tryptone soy agar (TSA) with 5% defibrinated sheep blood and 0.001% pyridoxal HCl. After 72-96 hours
176 of incubation, they form pinpoint transparent colonies morphologically indistinguishable from *H. ovis*
177 and displaying little to no alpha hemolysis. As shown in Figure 5, cryptic strain KG38 displays weak
178 hemolysis on blood agar when compared to *H. ovis* strains. In liquid medium, both *H. ovis* and the
179 cryptic strains grow well in brain heart infusion (BHI) broth supplemented with 0.1% Tween80 and
180 0.001% pyridoxal HCl.

181 As shown in Table 2, eight isolates were assessed to identify their enzymatic activity. *H. ovis*
182 strains KG36, KG37, KG104, and KG106, and cryptic strains KG38, KG95, 105, and KG197 exhibited
183 positive results for both alanine arylamidase and L-proline arylamidase. However, in contrast to the
184 cryptic strains, *H. ovis* strains also demonstrated positive results for at least one of the following:
185 tyrosine arylamidase (3/4), Beta galactopyranosidase (2/4), D-mannose (3/4), or D-maltose (1/4). Cryptic
186 strain KG38 was the sole strain positive for leucine arylamidase and alanyl-phenylalanyl-proline
187 arylamidase. Although the Vitek 2 Gram-Positive ID card is capable of identifying *Helcococcus kunzii*
188 based on its biochemical profile, it is not designed to identify *H. ovis*. As a result, all but one tested strain

189 produced "low confidence" or "unknown" species identification. Cryptic strain KG38 was misidentified as
190 99% probability "*Dermacoccus nishinomiyaensis*/*Kytococcus sedentarius*". These results indicate that
191 differentiating between *H. ovis* and the cryptic *Helcococcus* strains may be possible based on the
192 absence of specific enzymatic activity beyond alanine arylamidase and L-proline arylamidase. However,
193 a larger sample size is needed to draw any conclusions regarding the differential enzymatic activities of
194 these two clades.

195

196 **Table 2.** Biochemical characteristics and Vitek2 identification results of *Helcococcus* sp. isolates. Only
197 tests with at least one positive result are included. A complete list of biochemical tests is presented in
198 Supplemental File 4.

Isolate	APPA	LeuA	AlaA	ProA	TyrA	BGAR	dMAN	dMAL	Vitek2 ID
<i>Helcococcus ovis</i> KG104	-	-	+	+	+	+	-	-	Low Discrimination
<i>Helcococcus ovis</i> KG106	-	-	+	+	+	-	+	-	Low Discrimination
<i>Helcococcus ovis</i> KG36	-	-	+	+	-	+	+	-	Unidentified
<i>Helcococcus ovis</i> KG37	-	-	+	+	+	-	+	+	<i>Granulicatella elegans</i> (95% Probability)
<i>Helcococcus bovis</i> KG38	+	+	+	+	-	-	-	-	<i>Dermacoccus nishinomiyaensis</i> / <i>Kytococcus sedentarius</i> (99% Probability)
<i>Helcococcus bovis</i> KG95	-	-	+	+	-	-	-	-	Low Discrimination

<i>Helcococcus</i> <i>bovis</i> KG105	-	-	+	+	-	-	-	-	Low Discrimination
--	---	---	---	---	---	---	---	---	--------------------

<i>Helcococcus</i> <i>bovis</i> KG197	-	-	+	+	-	-	-	-	Low Discrimination
--	---	---	---	---	---	---	---	---	--------------------

199

200 ***H. ovis* Pangenome Construction and Associations**

201 The four genomes belonging to the cryptic strains were excluded from pangenomic analyses as this
202 study aims to explore the pangenome of *H. ovis*, the *Helcococcus* species associated with metritis in
203 dairy cows. A total of 31 genomes were initially included in the pangenome construction. However,
204 there were low-quality assemblies that did not result in complete enough genomes to warrant inclusion
205 into the pangenome. As shown in Figure 6, the number of new genes in the pan-genome plateaus after
206 25 genomes are included. We therefore excluded the five lowest-quality genome assemblies from the
207 pangenome construction and retained 26 assemblies in the analysis. The exclusion of these low-quality
208 assemblies resulted in the core genome expanding from 683 to 1045 gene families. The resulting core,
209 soft core, shell, and cloud genomes are shown in Figure 7. In short, the *H. ovis* pangenome consists of
210 845 core genes (99% <= strains <= 100%), 203 soft core genes (95% <= strains < 99%), 1078 shell genes
211 (15% <= strains < 95%), and 556 cloud genes (0% <= strains < 15%).
212 The final *H. ovis* pangenome includes 20 strains from cows with metritis and six strains from healthy
213 cows. The complete *H. ovis* pangenome, including the gene presence and absence table, is presented in
214 Supplemental File 5. We were interested in finding genes that were enriched in the metritis or healthy
215 group of strains. We ran a Scoary (20) analysis using both the 31-strain and the 26-strain pangenomes
216 with the Benjamini-Hochberg adjusted p-values to identify the genes most overrepresented in a specific
217 host group. Using a significance level of p<0.05 we did not find any gene group overrepresented in
218 either of the host groups.

219

220 **Virulome**

221 After using Abricate for mass screening of virulence factors in the 26 *H. ovis* genomes against the
222 Virulence Factor Database, no positive hits were returned. To further investigate the virulome of 26 *H.*
223 *ovis* strains in this study, we curated a set of 22 putative virulence factor genes based on previous
224 comparative genome analyses (15). The resulting virulome is presented in Figure 8 as a heat map. There
225 is no observable pattern in the presence or absence of virulence factors in these strains in relation to the
226 health status of the host or farm location.

227 Two hypothetical proteins and a pathogenicity island have been recognized as potential high virulence
228 determinants of *H. ovis* in invertebrate infection models (14). These high virulence determinant CDS are
229 found in 69% (18) of the strains in this study and are absent in only eight strains. Both the hypothetical
230 proteins and the pathogenicity island are co-occurring in every genome where they are present and are
231 altogether absent in the remaining strains. We used mauve to visually inspect the spatial distribution of
232 these co-occurring high virulence determinants in the two complete *H. ovis* genomes where they are
233 present. In both KG37 and KG106, the two hypothetical protein CDS are found closely associated with a
234 ZnuABC locus located more than 500,000 base pairs away from the co-occurring pathogenicity island. To
235 further explore the cause of the co-occurrence and co-absence of these virulence determinant CDS we
236 identified and excluded loci containing elevated densities of base substitutions in the twenty-six
237 genomes and built an approximately-maximum-likelihood phylogenetic tree (Supplemental File 6). The
238 clades that do not contain the high virulence determinant CDS seem to be spread across the tree,
239 showing that the co-occurring CDS are not restricted to a single lineage but are found in multiple, more
240 distantly related lineages.

241

242 **Resistome and Plasmids**

243 We also used Abricate for mass screening of acquired antimicrobial resistance genes (ARGs) against the
244 Comprehensive Antibiotic Resistance Database. The search was limited to acquired resistance genes
245 because not enough experimental data is available for *H. ovis* to evaluate resistance-associated point
246 mutations. We also screened for known plasmid sequences by querying against the PlasmidFinder
247 database. The results of these analyses are presented in Figure 9.

248 Strain KG107 is the only one of the thirty screened genomes that does not contain any acquired ARGs.
249 Nine *H. ovis* strains carry only *tetM*, 15 strains carry both *tetA* and *tetB*, and five strains carry both *tetT*
250 and *Inuc*. With the exception of *Inuc*, which confers resistance to lincosamides, all other ARGs found in
251 this experiment confer resistance to tetracyclines. Acquired antimicrobial resistance genes *tetA* and *tetB*
252 are, in all strains, located within a prophage region commonly found within *H. ovis* genomes. Similarly,
253 *tetT* and *InuC* are found in conjunction within a prophage region in all strains where they occur. This
254 suggests prophage integration events are a significant driver of ARGs acquisition in *H. ovis*. Alternatively,
255 *tetM* is located within a previously described integrated plasmid region (repUS43_1_CDS12738(DOp1)),
256 often found in *Streptococcus* spp.
257 A total of ten strains were selected to be evaluated for resistance to 22 clinically relevant antimicrobials.
258 Subsets of strains from each AMR genotype including *tetM* only (KG100, KG106, and KG113),
259 *tetA/tetB*(KG36, KG37, KG92, KG196), *tetT/lnuC* (KG104, KG109, KG120), and none (KG107), were
260 selected for minimum inhibitory concentration (MIC) testing. As shown in Table 3, MICs are reported in
261 µg/mL without antimicrobial resistance breakpoint interpretations because there are currently no
262 interpretive standards established by the Clinical and Laboratory Standards Institute (CLSI) for *H. ovis* in
263 the uterus of cattle. We used the MIC results of strain KG107 as the wild-type reference since it was the
264 only isolate that does not carry any known ARG. Strains carrying any tetracycline resistance gene (*tetT*,
265 *tetM*, or *tetA/tetB*) had a higher MIC for tetracycline. The wild-type strain had a tetracycline MIC \leq 0.250
266 µg/mL, and all other strains had a tetracycline MIC \geq 1.0 µg/mL. Although strains carrying *tetM* or *tetT*

267 displayed resistance to doxycycline and minocycline compared to the wild type, strains carrying
268 *tetA/tetB* did not follow the same pattern. None of the *tetA/tetB* positive strains had increased
269 resistance to minocycline, and their resistance to doxycycline was inconsistent and less than that of
270 *tetM* and *tetT* positive strains. Although MIC for lincomycin were not evaluated, the strains that carry
271 *InuC* (KG104, KG109, KG120) did not show resistance to clindamycin, the only lincosamide tested.

272

273 **Table 3.** Antimicrobial resistance profiles of *Helcococcus* sp. Minimum inhibitory concentration values
274 are in microgram/milliliter (µg/ml). The rows of tetracycline class antibiotics are highlighted in grey.

	<i>tetA/tetB</i>				<i>tetM</i>			<i>tetT/InuC</i>			none
	KG	KG	KG	KG	KG	KG	KG	KG	KG	KG	KG
	37	36	92	196	113	100	106	104	109	120	107
Amikacin	≤16	≤16	≤16	≤16	≤16	≤16	≤16	≤16	≤16	≤16	≤16
Amox/Clav	≤0.25	≤0.25	0.5	≤0.25	≤0.25	≤0.25	≤0.25	≤0.25	0.5	0.5	≤0.25
Ampicillin	≤0.25	≤0.25	0.5	≤0.25	≤0.25	≤0.25	≤0.25	≤0.25	0.5	0.5	≤0.25
Cefazolin	≤2	≤2	≤2	≤2	≤2	≤2	≤2	≤2	≤2	≤2	≤2
Cefovecin	2	2	4	1	1	1	0.5	2	4	4	0.5
Cefpodoxime	≤2	≤2	≤2	≤2	≤2	≤2	≤2	≤2	≤2	≤2	≤2
Cephalothin	≤2	≤2	≤2	≤2	≤2	≤2	≤2	≤2	≤2	≤2	≤2
Chloramphenicol	≤8	≤8	≤8	≤8	≤8	≤8	≤8	≤8	≤8	≤8	≤8
Clindamycin	≤0.5	≤0.5	≤0.5	≤0.5	≤0.5	≤0.5	≤0.5	≤0.5	≤0.5	≤0.5	≤0.5
Doxycycline	0.25	≤0.125	0.5	≤0.125	>0.5	>0.5	>0.5	>0.5	>0.5	>0.5	≤0.125
Enrofloxacin	≤0.25	≤0.25	≤0.25	≤0.25	0.25	≤0.25	≤0.25	≤0.25	≤0.25	≤0.25	≤0.25
Erythromycin	1	1	1	1	2	1	1	0.5	2	1	1
Gentamicin	≤4	≤4	≤4	≤4	≤4	≤4	≤4	≤4	≤4	≤4	≤4
Imipenem	≤1	≤1	≤1	≤1	≤1	≤1	≤1	≤1	≤1	≤1	≤1
Marbofloxacin	≤1	≤1	≤1	≤1	≤1	≤1	≤1	≤1	≤1	≤1	≤1
Minocycline	≤0.5	≤0.5	≤0.5	≤0.5	2	2	1	>2	>2	>2	≤0.5
Oxacillin	≤0.25	≤0.25	>2	>2	>2	>2	≤0.25	≤0.25	>2	>2	2
Penicillin	0.125	≤0.06	0.25	≤0.06	≤0.06	≤0.06	≤0.06	≤0.06	0.25	0.25	0.125
Rifampicin	≤1	≤1	≤1	≤1	≤1	≤1	≤1	≤1	≤1	≤1	≤1
Tetracycline	>1	>1	>1	1	1	>1	>1	>1	>1	>1	≤0.25
Trim./Sulfa	≤2	≤2	≤2	≤2	≤2	≤2	≤2	≤2	≤2	≤2	≤2
Vancomycin	≤1	≤1	≤1	≤1	≤1	≤1	≤1	≤1	≤1	≤1	≤1

275

276 Finally, as shown in Table 3, some strains showed resistance to cefovecin and oxacillin without
277 carrying any ARG known for conferring resistance to beta-lactams. We ran a Scoary (Brynilsrud et al.,
278 2016) analysis using a resistance threshold of ≥ 2 for cefovecin and ≥ 0.5 for oxacillin, using the CLSI soft-
279 tissue cutoffs for non-*Staphylococcus aureus* staphylococci in dogs and cats as an approximation (21).
280 We used the Benjamini-Hochberg adjusted p-values to identify the genes most overrepresented in a
281 specific host group. We did not find any gene group overrepresented in either of the host groups using a
282 significance level of $p < 0.05$. This suggests that beta-lactam resistance in *H. ovis* may be mediated by
283 chromosomal mutation resistance instead of mobile ARGs.

284

285 **Discussion**

286 In this study, we examined the genomes of *H. ovis* strains obtained from the uteri of both healthy dairy
287 cows and those with metritis. Our analysis focused on exploring the pangenome, resistome, virulome,
288 and taxonomic diversity of these strains. Additionally, we sought bacterial genome-wide associations
289 between *H. ovis* gene clusters and metritis in dairy cows.

290 While the costs of second-generation short-read whole-genome sequencing (WGS) have
291 significantly decreased in the past decade, third-generation long-read sequencing remains a less
292 affordable emerging technology. In our study, we opted for the more commonly used approach of
293 employing low-depth Illumina short-read sequencing to maximize the inclusion of a larger number of
294 strains in our analysis. As is evident in our findings, this approach may lead to the loss of genomes due
295 to low coverage and incomplete assemblies. However, this tradeoff is acceptable when considering the
296 low-cost, high-throughput generation of excellent-quality reads ($Q > 35$).

297 The *Helcococcus* genus is comprised of five well-described species. However, their genetic
298 diversity remains unexplored due to the limited availability of sequenced genomes. Within this small
299 genus there are still unresolved and contradictory taxonomic classifications. For example, the species *H.*

300 *pyogenes* was described as a new species isolated from a prosthetic joint infection based on biochemical
301 tests and a partial (518bp) 16S rRNA sequence identity in 2004 (2). A later study proposed another new
302 species, *H. seattlensis*, isolated from a human with urosepsis also based on 1512bp 16S rRNA sequence
303 identity, which also shares 99.4% sequence identity with *H. pyogenes* suggesting it is likely the same
304 species (3). Another taxonomic uncertainty within the genus is the classification of the *H. ovis* Tongji
305 strain, isolated from the only recorded *H. ovis* infection in a human (13). This strain displayed an atypical
306 biochemical profile for *H. ovis* and a 98.9% 16S rRNA sequence identity with the *H. ovis* type strain,
307 which led researchers to question its place within the species taxon. Phylogenomic analyses have shown
308 that, based on 16S rRNA sequence identity, the Tongji strain belongs to a subclade of the species also
309 populated by *H. ovis* strain KG38 (15). Whole genome-based multi-locus phylogenomic analyses in this
310 study confirmed these findings and identified three further strains (KG95, KG105, and KG197) belonging
311 to the cryptic clade. Average nucleotide identity, proteome identity, and phenotypic analyses provide
312 robust evidence that these strains belong to a distinct novel species, for which we propose the name *H.*
313 *bovis* sp. nov. (bo'vis. L. gen. n. bovis of the cow). *H. ovis* and *H. bovis* strains share 87-89% average
314 nucleotide identity with each other placing their relationship in the 0.2% of pairs that fall within the 83-
315 95% ANI valley range (22). This makes the relationship between the two species a rare candidate for
316 exploring bacterial speciation mechanisms and the role horizontal gene transfer has on the speciation
317 process. These *H. bovis* strains originated from two geographically separate farms in North Central
318 Florida. They were also retrieved from uteri of both cows with metritis (1) and healthy cows (3).
319 However, the sample size in this study is too small to draw conclusions about the association between
320 the presence of *H. bovis* and uterine health status. Strain KG38, part of the novel species group, has
321 been shown to have attenuated virulence when compared to other *H. ovis* isolates (14). Since *H. bovis*
322 occupies a similar biochemical niche as the more virulent *H. ovis* strains, its role as a commensal
323 organism of the reproductive tract is an area that warrants further exploration. Although the multiple

324 sequence alignment of the whole 16 S rRNA gene can discriminate between *H. ovis* and *H. bovis*, the
325 responsible sequence variations are in hypervariable regions V2 and V6 which are not often targeted in
326 metagenomic amplicon studies. This means sequences belonging to *H. bovis* will contribute reads to the
327 amplicon sequence variants classified as *H. ovis* in most metagenomic studies amplifying the V3-V4
328 hypervariable regions. Unlike the 16S rRNA sequence, *rpoB* has more regions of dissimilarity between *H.*
329 *ovis* and *H. bovis*, making it a much more useful single-marker gene to resolve these two *Helcococcus*
330 species.

331 We screened a subset of cows from this study to show that isolation of *H. ovis* from the uterus
332 of dairy cows is strongly associated with metritis. Previous studies have shown that *H. ovis* DNA is more
333 abundant in relative and absolute terms in the uterus of dairy cows with metritis than in healthy cows at
334 the time of metritis diagnosis (5,17). Although all healthy cows have been shown to harbor *H. ovis*
335 genomic DNA (gDNA) in the uterus after parturition, this gDNA is not indicative of the presence of viable
336 bacteria, likely because healthy cows are able to mount adequate immune responses that neutralize
337 these organisms (23,24). Previous to this study, isolation of live *H. ovis* from the uterus of dairy cows had
338 been limited to only cows with metritis, and targeted comparative cultivation screenings have not been
339 conducted (10,25). These results are a robust addition to the current body of evidence showing *H. ovis* is
340 one of the key organisms in the pathogenesis of metritis in dairy cows at the time of diagnosis.

341 Our inability to find any *H. ovis* genotype association with metritis is likely due to the fact that
342 metritis is characterized by a dysbiosis of the uterine microbiota that is unlikely to be explained by gene
343 groups within a single component bacterial species (18,26). Furthermore, as is the case in microbial
344 communities in gut dysbiosis, it is possible that *H. ovis* is more prevalent in the diseased uterus because
345 the disease condition widens an independent metabolic niche which the bacterium can then fill without
346 having to play a key role in the necessary steps for the development of disease (27). The genome-wide
347 association analyses conducted in this study have been successfully used to find the genetic basis for

348 high penetrance phenotypes in bacteria like virulence (28) or antimicrobial resistance (29), but we were
349 not able to establish any phenotype-genotype link with this approach. In this study we also measured
350 simple phenotypes like hemolysis and pyridoxal dependence in vitro for all strains but did not find any
351 insightful phenotypic variation between them.
352 Since *H. ovis* is not a well-known pathogen or a model organism, there is no experimentally verified
353 virulence factor (VF) data. We found that the putative pathogenicity island and the hypothetical VF
354 associated with a Zinc ABC transporter locus were either co-occurring or altogether absent from *H. ovis*
355 strains. Manual screening of the available complete genomes revealed that these putative VFs are not
356 part of the same operon in the species. This raises the question of whether they are functionally linked
357 or if they display this pattern in our samples by chance. As shown in Supplemental File 6, these putative
358 high virulence determinants are present and absent across different subclades of *H. ovis* and do not
359 show evidence of being driven by the founder effect. According to ProtelInfer (30), both the ZincABC
360 transporter-associated VF and the conserved membrane-spanning protein within the pathogenicity
361 island participate in metal ion binding and transport. This suggests that, as has been shown in
362 *Escherichia coli* (31), these *H. ovis* accessory virulence genes co-occur due to having connected
363 functions, and the resulting phylogenetic distributions are the result of convergent gene loss instead of
364 founder effect.

365 All the ARGs found in our strains are located within mobile genetic elements like plasmids or
366 prophage regions, which makes *H. ovis* a reservoir of mobile ARGs in a food production setting. All but
367 one *H. ovis* strain (KG107) contain ARGs conferring resistance to tetracyclines. This strain is a valuable
368 clinical isolate since it can be used as a wild-type reference strain with no ARGs to benchmark the
369 susceptibility of *H. ovis* to antimicrobials. Unlike *tetA/tetB* positive strains, strains carrying genes
370 encoding the cytoplasmic ribosomal protection proteins TetM or TetT, also have elevated resistance to
371 doxycycline and minocycline. Oxytetracycline and ceftiofur are the only two antimicrobials labeled in the

372 United States for the treatment of metritis in lactating dairy cattle. However, the United States Food and
373 Drug Administration has banned the extra-label use of ceftiofur in animals, and may move towards
374 policies like the Netherlands where the use of ceftiofur administration to agricultural animals is
375 restricted (32). The alternative, intrauterine oxytetracycline infusions, remains a frequent practice both
376 in clinical and research settings in the United States and Europe (33,34). Furthermore, dairy operations
377 often use oxytetracycline as prophylactics in heifer rearing or as a treatment for calf pneumonia, a type
378 of infection *H. ovis* has been implicated in (12). Although the MICs for oxytetracycline were not
379 assessed, there is no inherent difference between a tetracycline and an oxytetracycline resistance genes
380 (35), and 96.8% of isolates in this study carry at least one tetracycline resistance gene shown to confer
381 tetracycline resistance in vitro. These findings indicate that further studies are needed to evaluate the
382 effectiveness of tetracyclines as a treatment for metritis in dairy cattle.

383

384 Conclusion

385 This study found that the presence of viable *H. ovis* in the uterus of dairy cows is associated with
386 metritis. However, we found no evidence that a specific *H. ovis* genotype or gene cluster is associated
387 with the disease. Virulence factor comparisons showed two putative high virulence determinants are
388 common but have varying prevalence in these strains with a phylogenetic distribution consistent with
389 convergent gene loss. Based on the genetic dissimilarity and phenotypic characteristics, strains KG38,
390 KG95, KG105 and KG197 represent a novel species of the genus *Helcococcus*, for which we propose the
391 name *Helcococcus bovis* sp. Nov. (bo'vis. L. gen. n. bovis of the cow). The type strain for this species is
392 KG38 (Accession number CP121192). The significance of this species in the context of uterine health
393 remains to be explored. The majority (30/31) of *H. ovis* strains in this study carry antimicrobial resistance
394 genes conferring resistance to tetracyclines, which has significant clinical consequences for the
395 treatment of metritis and other *H. ovis*-associated respiratory infections in cattle. The convergence of

396 widespread ARG-mediated tetracycline resistance in these uterine pathogens and initiatives to phase
397 out the use of ceftiofur to treat metritis reveals an immediate need to find alternative treatments and
398 prevention strategies for this important animal disease.

399

400 **Materials and Methods**

401 **Metritis Diagnosis and Uterine Sample Collection**

402 All procedures involving cows were approved by the Institutional Animal Care and Use Committee of the
403 University of Florida; protocol number 201910623. In this study, a total of 43 lactating Holstein Friesian
404 cows were used. Three cows were from North Florida Holsteins and 40 were from the University of
405 Florida's Dairy Research Unit, both located in north central Florida. Each cow had uterine discharge
406 collected directly from the uterus with a sterile pipette, and evaluated at four, six, and eight days
407 postpartum. 500uL of uterine discharge was suspended in 500uL of BHI broth with 30% glycerol and
408 stored at -80 °C.

409 The uterine discharge was scored on a 5-point scale (Jeon et al., 2016). Score 1 indicates normal lochia,
410 viscous, clear, red, or brown discharge that was not fetid; Score 2 indicates cloudy mucoid discharge
411 with flecks of pus; Score 3 indicates mucopurulent discharge that was not fetid with less than 50% pus;
412 Score 4 indicates mucopurulent discharge that was not fetid with more than 50% pus; and Score 5
413 indicates fetid red-brownish, watery discharge. Cows with uterine discharge scores of 1-4 were
414 considered healthy, whereas those with a score of 5 were diagnosed with metritis. Nine cows that had a
415 uterine discharge score of 1 to 4 at the time of sampling but developed metritis sometime in the 21 days
416 after parturition were excluded from microbiological testing.

417

418 **Bacteria Isolation and Identification**

419 To selectively culture *H. ovis* from uterine discharge samples, 20µL of the discharge suspension was
420 streaked onto *Helcococcus* selective agar. The agar plates were incubated for 72 hours at 36°C under
421 aerobic conditions with 6% CO₂ (11). Following incubation, individual pinpoint nonpigmented colonies
422 were selected and sub-cultured on tryptone soy agar with 5% defibrinated sheep blood and 0.001%
423 pyridoxal HCl for propagation. Species determination of the isolates was performed via comparative
424 analysis of Sanger sequencing of their 16S rRNA genes.

425

426 **Whole Genome Sequencing**

427 Genomic DNA (gDNA) was extracted using the DNeasy blood and tissue kit following the manufacturer's
428 instructions (Qiagen). Genomic DNA purity was measured using a NanoDrop 2000 spectrophotometer;
429 final DNA concentration was confirmed with a Qubit 2.0 Fluorometer. DNA integrity was visualized via
430 agarose gel electrophoresis. Library preparation was done with the Nextera XT kit (Illumina, Inc.),
431 following the manufacturer's instructions, and it was loaded into the MiSeq reagent kit V2. Sequencing
432 was performed on a MiSeq platform (Illumina, Inc.) with a 2 × 250-bp 500-cycle cartridge. Seven
433 previously sequenced strains were also included in this study. Two of them consist of Illumina
434 sequenced draft genomes KG39 (Accession number SRX5460741) and KG40 (Accession number
435 SRX5460742). The remaining five are complete genomes that were hybrid assembled using ONT and
436 Illumina sequencing for genomic comparisons performed in a previous study (15) (KG36, KG36, KG38,
437 KG104, KG106).

438

439 **Genome Assembly and Annotation**

440 After performing quality control with fastp (36) the resulting reads were evaluated using MultiQC
441 (v1.14). The minimum coverage threshold for inclusion in the study was set at 15x (37). De-novo genome
442 assembly was performed using Unicycler (v0.5.0) (38). Assembly quality was assessed using

443 Benchmarking Universal Single-Copy Orthologs (v4.1.2) (39). Genome annotations were conducted using

444 Prokka and the genome annotation service in BV-BRC using the RAST tool kit (40,41)

445

446 **Taxonomic analyses**

447 Whole genomes of *Helcococcus* spp. and the type strains of the recognized species within the genera

448 *Helcococcus*, *Finegoldia*, and *Parvimonas* were used to create a phylogenetic tree with the BV-BRC

449 codon tree pipeline using 500 single-copy PGFams (42). In order to verify that the constructed

450 phylogenetic tree was not affected by recombination events, we used Snippy (v4.6.0) to align Illumina

451 reads of the 26 *H. ovis* genomes using the *H. ovis* KG37 complete genome assembly as reference (43).

452 We then used Gubbins (v3.3.3) to identify loci affected by recombination and construct a phylogeny

453 based on point mutations outside of these regions (44). Phylogenetic trees were visualized and

454 annotated using Interactive Tree of Life (iTOL v5) webtool (45). Average nucleotide identities (ANI) were

455 calculated via BLAST pair-wise comparisons of all sequences shared between two strains (ANIb) using

456 the JSpecies web server (Richter et al., 2016). 16S rRNA gene sequences were extracted from the raw

457 paired-end Illumina reads using phyloFlash (v3.4.2) and *rpoB* genes were extracted from the trycycler-

458 assembled contigs using the BV-BRC Comparative Systems Service (42). Extracted nucleotide sequences

459 were aligned using Mafft (v7) and visualized on the BV-BRC Multiple Sequence Alignment and SNP /

460 Variation Analysis Service (42,46).

461

462 **Phenotype testing of select isolates**

463 The biochemical profile and antimicrobial susceptibility phenotype of a subset of isolates was assessed

464 at the University of Georgia College of Veterinary Medicine Athens Veterinary Diagnostics Laboratory.

465 using the Vitek2 Gram-positive bacteria ID card for biochemical tests and the Sensititre COMPGP1F

466 plates (ThermoFisher) for MIC testing, according to the manufacturers' instructions.

467 For MICs, we inoculated sterile H₂O with *H. ovis* to achieve a 0.5 McFarland; 10 uL of the inoculum was
468 added to 10 mls of Mueller-Hinton broth containing lysed horse blood and supplemented with 0.1 mg of
469 pyridoxal HCL. Finally, 50 uLs of the Mueller-Hinton broth containing *H. ovis* were aliquoted into each
470 well of the Sensititre plate, incubated at 35C in aerobic conditions, and read at 24 and 48 hours.
471 For biochemical testing on the Vitek2 system, we inoculated 0.45% saline with *H. ovis* to achieve a 0.5
472 McFarland and entered the cards into the Vitek2 system. The Vitek2 system then made the appropriate
473 dilutions and automatically read them at 15-minute intervals until completed, which was 5 to 8 hours,
474 depending on the isolate. We opted to use the Gram-positive ID card because it contains all of the
475 biochemical tests used to identify *H. ovis* in previous studies (13). For biochemical testing, we selected
476 the 4 *H. ovis* strains with complete genome assemblies (KG36, KG37, KG104, and KG106) and the 4
477 *Helcococcus* cryptic strains (KG38, KG95, KG105, KG197). For antimicrobial sensitivity testing, we
478 selected 10 *H. ovis* strains representing each tetracycline resistance gene profile including *tetM* only
479 (KG100, KG106, and KG113), *tetA/tetB*(KG36, KG92, KG196), *tetT* only (KG104, KG109, KG120), and none
480 (KG107).
481

482 **Pangenome Analysis**
483 The *H. ovis* pangenome was constructed using Roary with default parameters and gene clusters were
484 annotated using the BV-BRC Comparative Systems Service (42). To identify gene clusters associated with
485 metritis, we used Scoary with default parameters (20). Scoary identifies gene presence or absence
486 variants significantly associated with a trait by performing Fisher's Exact Tests. It then uses the
487 phylogenetic relations between strains to look for the causal set of genes. Causal genes were defined as
488 those with Bonferroni-corrected p-values < 0.05.
489

490 **Virulome and Resistome**

491 Abricate was used to screen all assembled genomes for ARGs using the NCBI AMRFinder and CARD
492 databases (github.com/tseemann/abricate) (47,48). ARGs associated with point mutations were
493 excluded due to a lack of experimental data for the *Helcococcus* genus. Abricate was also used to screen
494 for virulence factors against the VFDB for known plasmids against the PlasmidFinder database (49,50).
495 Virulence factors were further manually searched for using the BV-BRC Comparative Systems Service
496 (42).

497

498 **Figures**

499 **Figure 1.** Heat map of whole genome average nucleotide identity based on BLAST+ (ANib) and
500 maximum-likelihood phylogenetic tree of 35 *Helcococcus* strains included in this study. The clade
501 colored in red represents cryptic *Helcococcus* clade.

502 **Figure 2.** Heat map of whole genome average nucleotide identity based on BLAST+ (ANib) and
503 maximum-likelihood phylogenetic tree of the selected genomes of *Helcococcus ovis* and *Helcococcus*
504 *bovis*, the type strains of the remaining species of the *Helcococcus* genus, and the type species of the
505 most closely related genera to *Helcococcus*, *Finegoldia* and *Parvimonas*. [T] denotes the genome of a
506 type organism.

507 **Figure 3.** A) Multiple sequence alignment and sequence entropy plot of near-complete *Helcococcus ovis*
508 16S rRNA from this study, the *Helcococcus ovis* Tongji strain, and the *Helcococcus ovis* type strain. B)
509 Multiple sequence alignment and sequence entropy plot of *rpoB* sequences from this study. Alignment
510 windows display examples of areas of sequence entropy that can be used to differentiate between
511 *Helcococcus ovis* and *Helcococcus bovis*.

512 **Figure 4.** Circos plot of protein sequence alignments of three *Helcococcus ovis* and three *Helcococcus*
513 *bovis* strains. Percent protein sequence identities were calculated against the proteome of reference
514 strain *Helcococcus ovis* KG36.

515 **Figure 5.** Examples of *Helcococcus ovis* KG37 (A) and *Helcococcus bovis* KG38 (B) culture on tryptone soy
516 agar with 5% defibrinated sheep's blood and 0.001% pyridoxal HCl after 72 hours of incubation.

517 **Figure 6.** Plots depicting how the pangenome varies as genomes are randomly added to the pangenome
518 construction. The dashed blue line marks the 25-genome threshold selected for this study.

519 **Figure 7.** A) *Helcococcus ovis* pangenome gene matrix depicting the 2682 gene clusters identified by
520 Roary. B) Pangenome frequency plot depicting how many gene clusters are found in only 1 to only 25
521 genomes. C) Pie chart summarizing the pangenome structure.

522 **Figure 8.** Heat map of virulence factors of *Helcococcus ovis* strains explored in this study.

523 **Figure 9.** Heat map of antimicrobial resistance gene profiles of *Helcococcus ovis* strains sequenced in this
524 study.

525 **Data Availability**

526 The whole-genome sequences and the trimmed reads have been uploaded into the NCBI Sequence Read
527 Archive and are found under BioProject number PRJNA514352. SRA accession numbers for the trimmed
528 reads are listed in Supplemental File 2. GenBank accession numbers for the genome assemblies are
529 listed in Supplemental File 3.

530 **Ethics Declarations**

531 Experimental procedures involving cows were performed in accordance with relevant guidelines and
532 regulations and were approved by the Institutional Animal Care and Use Committee of the University of
533 Florida, under protocol number 201910623. The authors declare no competing interests.

534

535 **References**

536 1. Collins MD, Facklam RR, Rodrigues UM, Ruoff KL. Phylogenetic Analysis of Some Aerococcus-Like
537 Organisms from Clinical Sources: Description of *Helcococcus kunzii* gen. nov., sp. nov. International
538 Journal of Systematic Bacteriology. 1993 Jul 1;43(3):425–9.

539 2. Panackal AA, Houze YB, Prentice J, Leopold SS, Cookson BT, Liles WC, et al. Prosthetic Joint Infection
540 Due to “*Helcococcus pyogenica*.” J Clin Microbiol. 2004 Jun;42(6):2872–4.

541 3. Chow SK, Clarridge JE. Identification and Clinical Significance of *Helcococcus* species, with
542 Description of *Helcococcus seattlensis* sp. nov. from a Patient with Urosepsis. Forbes BA, editor. J
543 Clin Microbiol. 2014 Mar;52(3):854–8.

544 4. Fall NS, Raoult D, Sakhna C, Lagier JC. ‘*Helcococcus massiliensis*’ sp. nov., a new bacterial species
545 isolated from the vaginal sample of a woman with bacterial vaginosis living in Dielmo, Senegal. New
546 Microbes and New Infections. 2018 Sep;25:27–9.

547 5. Cunha F, Jeon SJ, Daetz R, Vieira-Neto A, Laporta J, Jeong KC, et al. Quantifying known and emerging
548 uterine pathogens, and evaluating their association with metritis and fever in dairy cows.
549 Theriogenology. 2018;114:25–33.

550 6. Liu K, Deng Z, Zhang L, Gu X, Liu G, Liu Y, et al. Biological Characteristics and Pathogenicity of
551 *Helcococcus ovis* Isolated From Clinical Bovine Mastitis in a Chinese Dairy Herd. Front Vet Sci. 2022
552 Feb 11;8:756438.

553 7. García A, Risco D, Benítez JM, Martínez R, García WL, Cuesta JM, et al. *Helcococcus ovis* isolated
554 from a goat with purulent bronchopneumonia and pulmonary abscesses. J VET Diagn Invest. 2012
555 Jan;24(1):235–7.

556 8. Collins MD, Faken E, Foster G, Monasterio LR, Dominguez L, Fernandez-Garazabal JF. NOTE
557 *Helcococcus ovis* sp . nov ., a Gram-positive organism from sheep. International Journal of
558 Systematic Bacteriology. 1999;49(1 999):1429–32.

559 9. Bilk S, Nordhoff M, Schulze C, Wieler LH, Kutzer P. Antimicrobial susceptibilities and occurrence of
560 resistance genes in bovine *Helcococcus ovis* isolates. Vet Microbiol. 2011;149(3–4):488–91.

561 10. Locatelli C, Scaccabarozzi L, Pisoni G, Bronzo V, Casula A, Testa F, et al. *Helcococcus kunzii* and
562 *Helcococcus ovis* isolated in dairy cows with puerperal metritis. 2013;374(NOVEMBER).

563 11. Kutzer P, Brunnberg L, Wieler LH, Gruber A, Staufenbiel R. Investigations on the occurrence of
564 *Helcococcus ovis* in bovine valvular endocarditis and phenotypic characterization and susceptibility
565 testing of the isolates. PhD dissertation. Freie Universität Berlin, Berlin, Germany (in German with
566 English abstract). 2009.

567 12. Jost A, Sickinger M. *Helcococcus ovis* associated with septic arthritis and bursitis in calves – a case
568 report. BMC Vet Res. 2021 Dec;17(1):291.

569 13. Mao L, Chen Z, Lu Y, Yu J, Zhou Y, Lin Q, et al. *Helcococcus ovis* in a patient with an artificial eye: a
570 case report and literature review. BMC Infect Dis. 2018 Dec;18(1):401.

571 14. Cunha F, Burne A, Casaro S, Brown MB, Bisinotto RS, Galvao KN. Establishing *Galleria mellonella* as
572 an invertebrate model for the emerging multi-host pathogen *Helcococcus ovis*. *Virulence*. 2023 Dec
573 31;14(1):2186377.

574 15. Cunha F, Casaro S, Jones KL, Bisinotto RS, Kariyawasam S, Brown MB, et al. Sequencing and
575 characterization of *Helcococcus ovis*: a comprehensive comparative genomic analysis of virulence.
576 *BMC Genomics*. 2023 Aug 30;24(1):501.

577 16. Pérez-Báez J, Silva TV, Risco CA, Chebel RC, Cunha F, De Vries A, et al. The economic cost of metritis
578 in dairy herds. *Journal of Dairy Science*. 2021 Mar;104(3):3158–68.

579 17. Jeon SJ, Vieira-Neto A, Gobikrushanth M, Daetz R, Mingoti RD, Parize ACB, et al. Uterine microbiota
580 progression from calving until establishment of metritis in dairy cows. *Applied and Environmental
581 Microbiology*. 2015;81(July):AEM.01753-15.

582 18. Jeon SJ, Galvão KN. An Advanced Understanding of Uterine Microbial Ecology Associated with
583 Metritis in Dairy Cows. *Genomics Inform*. 2018 Dec 31;16(4):e21.

584 19. Williamson CHD, Stone NE, Nunnally AE, Roe CC, Vazquez AJ, Lucero SA, et al. Identification of novel,
585 cryptic *Clostridioides* species isolates from environmental samples collected from diverse
586 geographical locations. *Microbial Genomics* [Internet]. 2022 Feb 23 [cited 2024 Feb 3];8(2).
587 Available from:
588 <https://www.microbiologyresearch.org/content/journal/mgen/10.1099/mgen.0.000742>

589 20. Brynildsrud O, Bohlin J, Scheffer L, Eldholm V. Rapid scoring of genes in microbial pan-genome-wide
590 association studies with Scoary. *Genome Biol*. 2016 Dec;17(1):238.

591 21. Performance Standards for Antimicrobial Disk and Dilution Susceptibility Tests for Bacteria Isolated
592 From Animals. 6th ed. 2024. 164 p.

593 22. Jain C, Rodriguez-R LM, Phillip AM, Konstantinidis KT, Aluru S. High throughput ANI analysis of 90K
594 prokaryotic genomes reveals clear species boundaries. *Nat Commun*. 2018 Nov 30;9(1):5114.

595 23. Martinez N, Sinedino LDP, Bisinotto RS, Ribeiro ES, Gomes GC, Lima FS, et al. Effect of induced
596 subclinical hypocalcemia on physiological responses and neutrophil function in dairy cows. *Journal
597 of Dairy Science*. 2014 Feb;97(2):874–87.

598 24. Jeon SJ, Cunha F, Ma X, Martinez N, Vieira-Neto A, Daetz R, et al. Uterine microbiota and immune
599 parameters associated with fever in dairy cows with metritis. *PLoS ONE*. 2016;11(11).

600 25. Cunha F, Jeon SJ, Kutzer P, Jeong KC, Galvão KN. Draft genome sequences of *helcococcus ovis* strains
601 isolated at time of metritis diagnosis from the uterus of holstein dairy cows. *Microbiology Resource
602 Announcements*. 2019;8(22).

603 26. Gomez DE, Galvao KN, Rodriguez-Lecompte JC, Costa MC. The Cattle Microbiota and the Immune
604 System An Evolving Field. *VETERINARY CLINICS OF NORTH AMERICA-FOOD ANIMAL PRACTICE*.
605 2019;35(3):485-+.

606 27. Watson AR, Füssel J, Veseli I, DeLongchamp JZ, Silva M, Trigodet F, et al. Metabolic independence
607 drives gut microbial colonization and resilience in health and disease. *Genome Biol.* 2023 Apr
608 17;24(1):78.

609 28. Laabei M, Recker M, Rudkin JK, Aldeljawi M, Gulay Z, Sloan TJ, et al. Predicting the virulence of
610 MRSA from its genome sequence. *Genome Res.* 2014 May;24(5):839–49.

611 29. Ellington MJ, Heinz E, Wailan AM, Dorman MJ, De Goffau M, Cain AK, et al. Contrasting patterns of
612 longitudinal population dynamics and antimicrobial resistance mechanisms in two priority bacterial
613 pathogens over 7 years in a single center. *Genome Biol.* 2019 Dec;20(1):184.

614 30. Sanderson T, Bileschi ML, Belanger D, Colwell LJ. ProtelInfer, deep neural networks for protein
615 functional inference. *eLife.* 2023 Feb 27;12:e80942.

616 31. Hall RJ. Gene-gene relationships in an *Escherichia coli* pangenome are linked to function and
617 mobility. 2021 Mar 25 [cited 2024 Mar 26]; Available from:
618 <https://rdmc.nottingham.ac.uk/handle/internal/9129>

619 32. Kuipers A, Koops WJ, Wemmenhove H. Antibiotic use in dairy herds in the Netherlands from 2005 to
620 2012. *Journal of Dairy Science.* 2016 Feb;99(2):1632–48.

621 33. Haimerl P, Arlt S, Borchardt S, Heuwieser W. Antibiotic treatment of metritis in dairy cows—A meta-
622 analysis. *Journal of Dairy Science.* 2017 May;100(5):3783–95.

623 34. Mileva R, Karadaev M, Fasulkov I, Ruseanova N, Vasilev N, Milanova A. Oxytetracycline Persistence in
624 Uterine Secretion after Intrauterine Administration in Cows with Metritis. *Animals.* 2022 Jul
625 28;12(15):1922.

626 35. Chopra I, Roberts M. Tetracycline Antibiotics: Mode of Action, Applications, Molecular Biology, and
627 Epidemiology of Bacterial Resistance. *Microbiol Mol Biol Rev.* 2001 Jun;65(2):232–60.

628 36. Chen S, Zhou Y, Chen Y, Gu J. fastp: an ultra-fast all-in-one FASTQ preprocessor. *Bioinformatics.*
629 2018 Sep 8;34(12):i884–90.

630 37. Bogaerts B, Winand R, Van Braekel J, Hoffman S, Roosens NHC, De Keersmaecker SCJ, et al.
631 Evaluation of WGS performance for bacterial pathogen characterization with the Illumina
632 technology optimized for time-critical situations. *Microbial Genomics* [Internet]. 2021 Nov 5 [cited
633 2023 Jun 7];7(11). Available from:
634 <https://www.microbiologyresearch.org/content/journal/mgen/10.1099/mgen.0.000699>

635 38. Wick RR, Judd LM, Gorrie CL, Holt KE. Unicycler: Resolving bacterial genome assemblies from short
636 and long sequencing reads. Phillippy AM, editor. *PLoS Comput Biol.* 2017 Jun 8;13(6):e1005595.

637 39. Manni M, Berkeley MR, Seppey M, Simão FA, Zdobnov EM. BUSCO Update: Novel and Streamlined
638 Workflows along with Broader and Deeper Phylogenetic Coverage for Scoring of Eukaryotic,
639 Prokaryotic, and Viral Genomes. Kelley J, editor. *Molecular Biology and Evolution.* 2021 Sep
640 27;38(10):4647–54.

641 40. Seemann T. Prokka: rapid prokaryotic genome annotation. *Bioinformatics*. 2014 Jul 15;30(14):2068–
642 9.

643 41. Brettin T, Davis JJ, Disz T, Edwards RA, Gerdes S, Olsen GJ, et al. RASTtk: A modular and extensible
644 implementation of the RAST algorithm for building custom annotation pipelines and annotating
645 batches of genomes. *Scientific Reports*. 2015;5.

646 42. Olson RD, Assaf R, Brettin T, Conrad N, Cucinell C, Davis JJ, et al. Introducing the Bacterial and Viral
647 Bioinformatics Resource Center (BV-BRC): a resource combining PATRIC, IRD and ViPR. *Nucleic Acids*
648 *Research*. 2023 Jan 6;51(D1):D678–89.

649 43. Seemann T. snippy: fast bacterial variant calling from NGS reads. 2015; Available from:
650 <https://github.com/tseemann/snippy>

651 44. Croucher NJ, Page AJ, Connor TR, Delaney AJ, Keane JA, Bentley SD, et al. Rapid phylogenetic
652 analysis of large samples of recombinant bacterial whole genome sequences using Gubbins. *Nucleic*
653 *Acids Research*. 2015 Feb 18;43(3):e15–e15.

654 45. Letunic I, Bork P. Interactive Tree Of Life (iTOL) v5: an online tool for phylogenetic tree display and
655 annotation. *Nucleic Acids Research*. 2021 Jul 2;49(W1):W293–6.

656 46. Katoh K. MAFFT: a novel method for rapid multiple sequence alignment based on fast Fourier
657 transform. *Nucleic Acids Research*. 2002 Jul 15;30(14):3059–66.

658 47. Jia B, Raphenya AR, Alcock B, Waglechner N, Guo P, Tsang KK, et al. CARD 2017: expansion and
659 model-centric curation of the comprehensive antibiotic resistance database. *Nucleic Acids Res.* 2017
660 Jan 4;45(D1):D566–73.

661 48. Feldgarden M, Brover V, Haft DH, Prasad AB, Slotta DJ, Tolstoy I, et al. Validating the AMRFinder
662 Tool and Resistance Gene Database by Using Antimicrobial Resistance Genotype-Phenotype
663 Correlations in a Collection of Isolates. *Antimicrob Agents Chemother*. 2019 Nov;63(11):e00483-19.

664 49. Carattoli A, Zankari E, García-Fernández A, Voldby Larsen M, Lund O, Villa L, et al. *In Silico* Detection
665 and Typing of Plasmids using PlasmidFinder and Plasmid Multilocus Sequence Typing. *Antimicrob*
666 *Agents Chemother*. 2014 Jul;58(7):3895–903.

667 50. Chen L, Zheng D, Liu B, Yang J, Jin Q. VFDB 2016: hierarchical and refined dataset for big data
668 analysis—10 years on. *Nucleic Acids Res.* 2016 Jan 4;44(D1):D694–7.

669

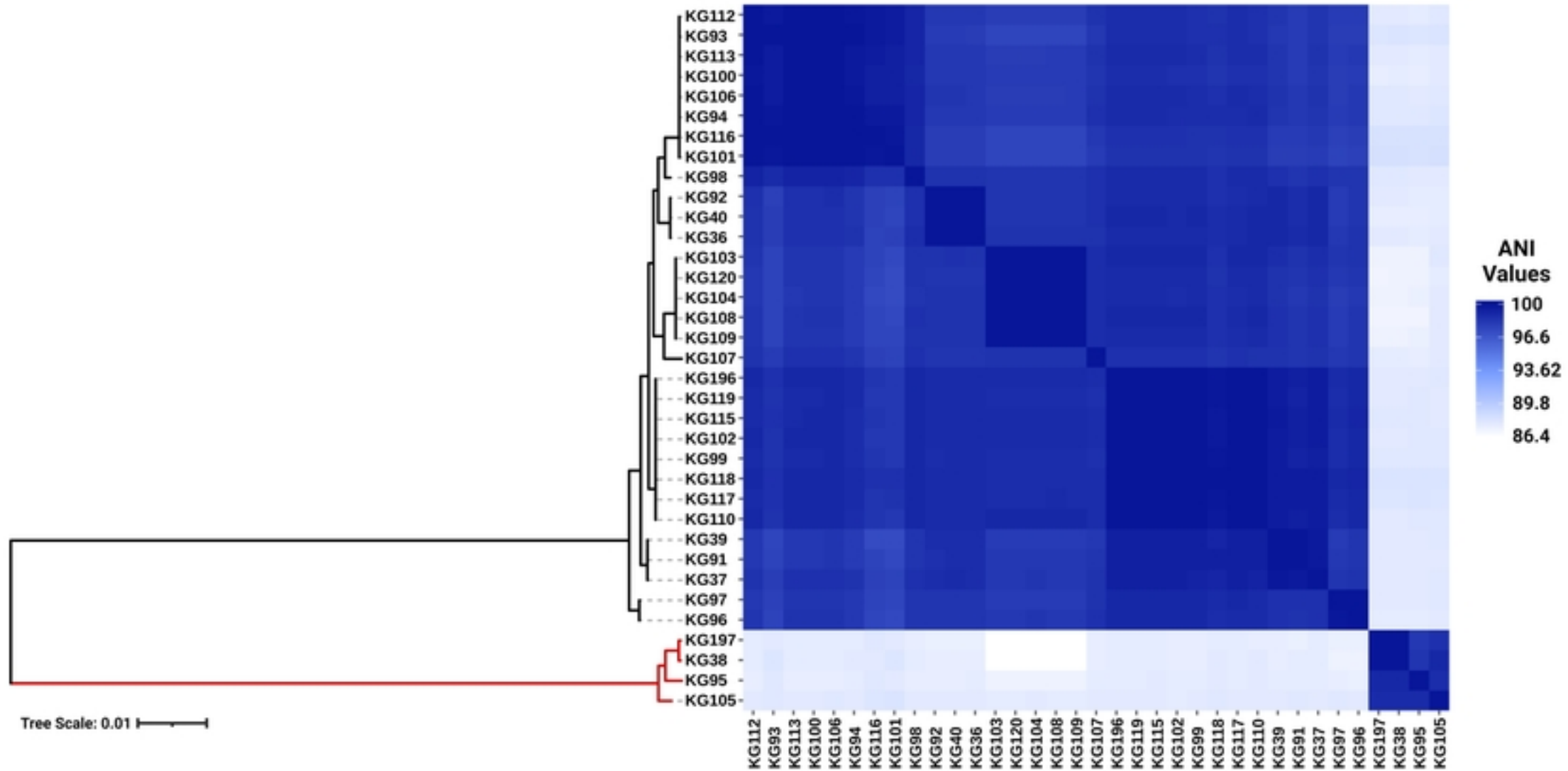


Figure 1

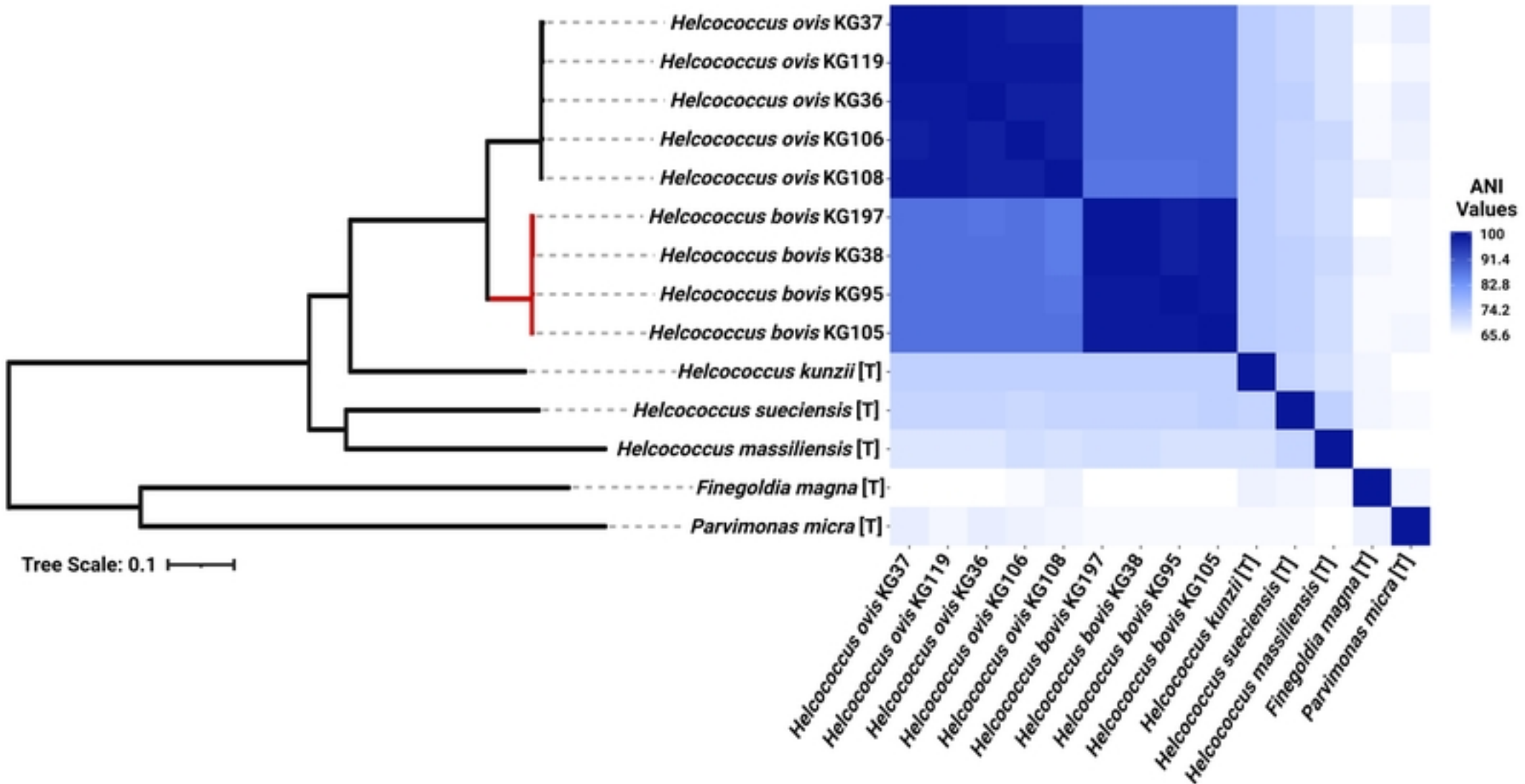
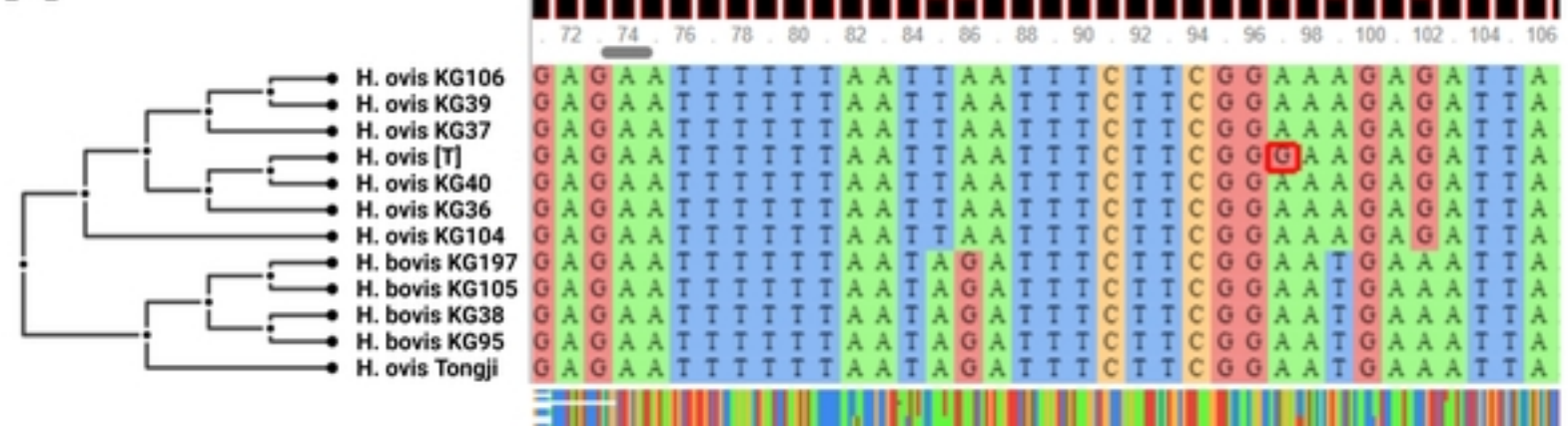
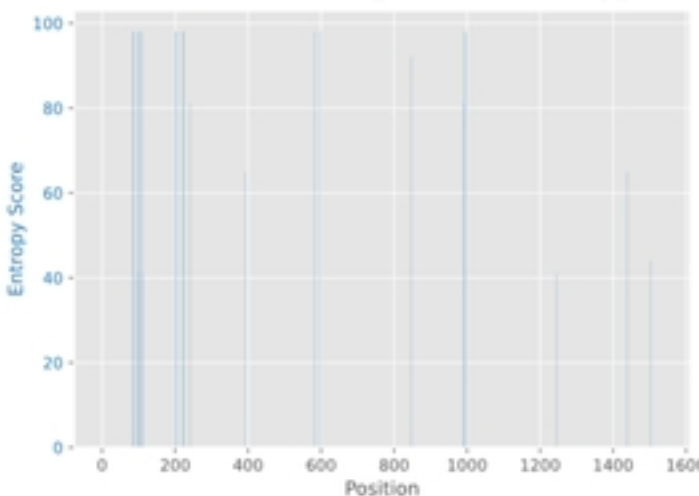
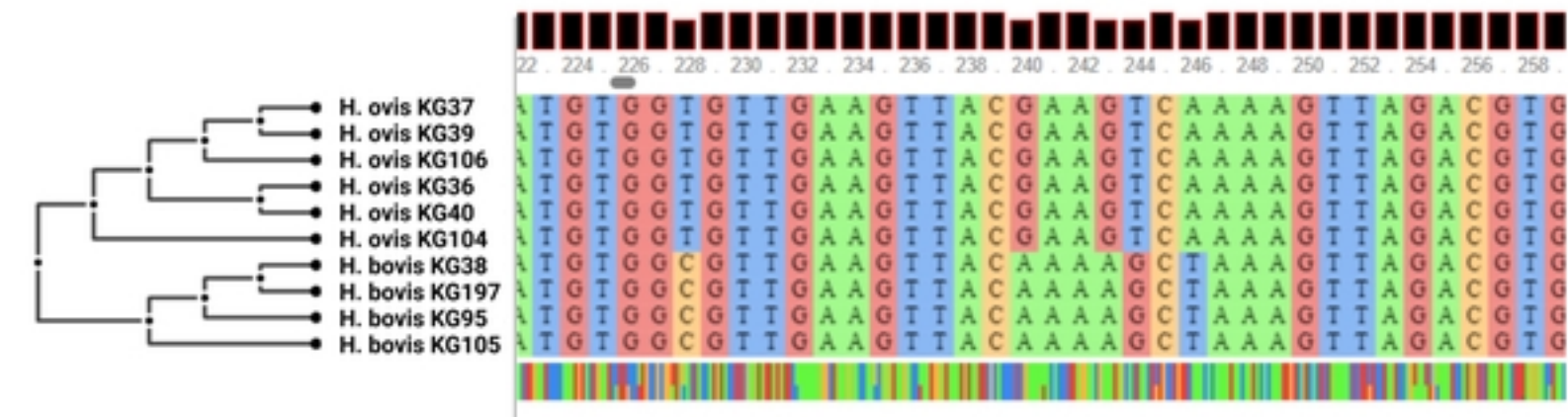
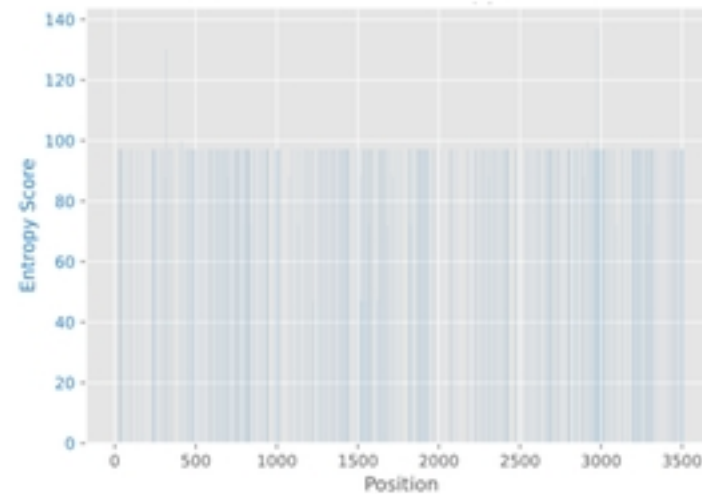


Figure 2

A**16S rRNA Alignment Entropy****B****rpoB Alignment Entropy****Figure 3**

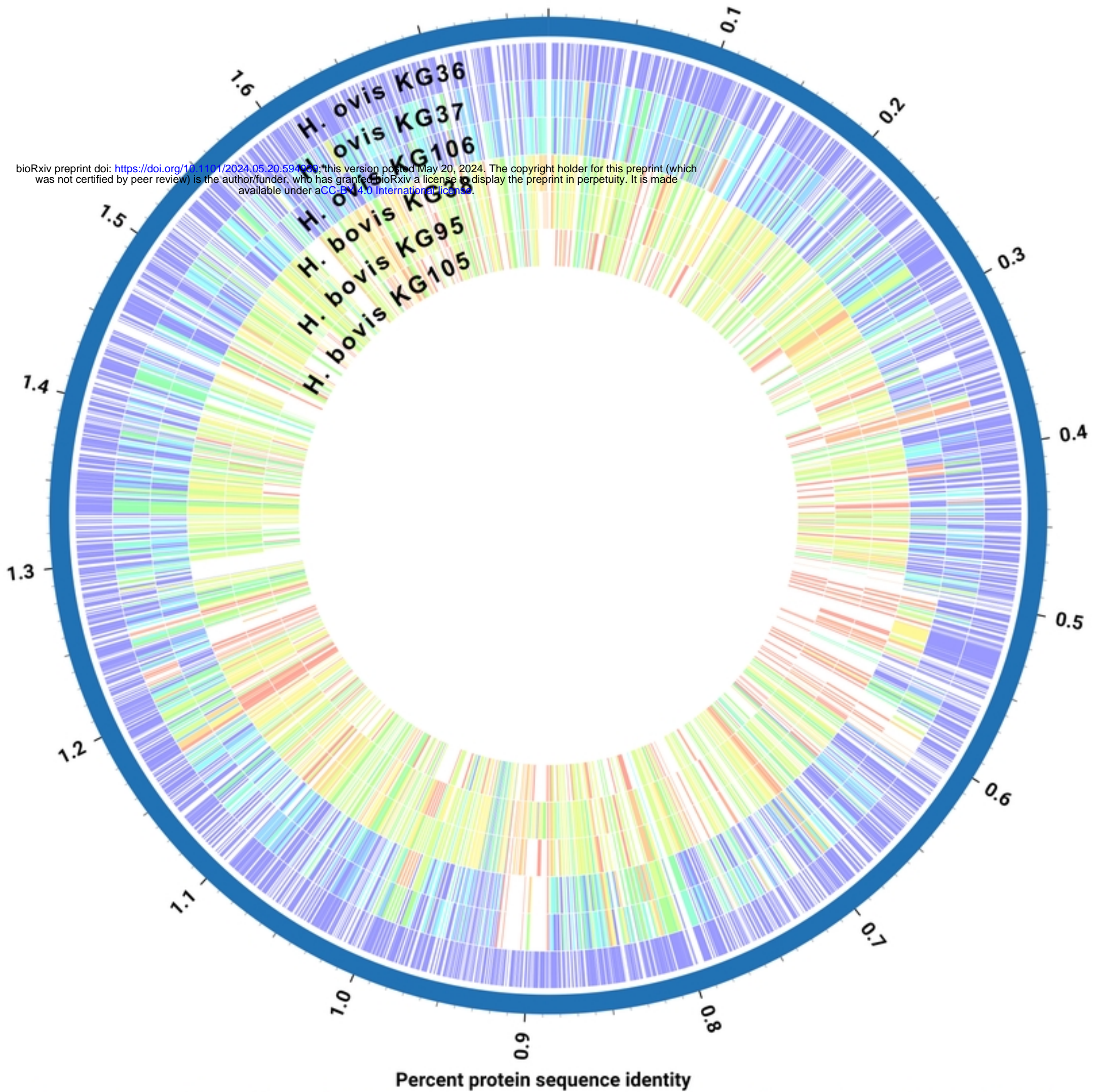


Figure 4

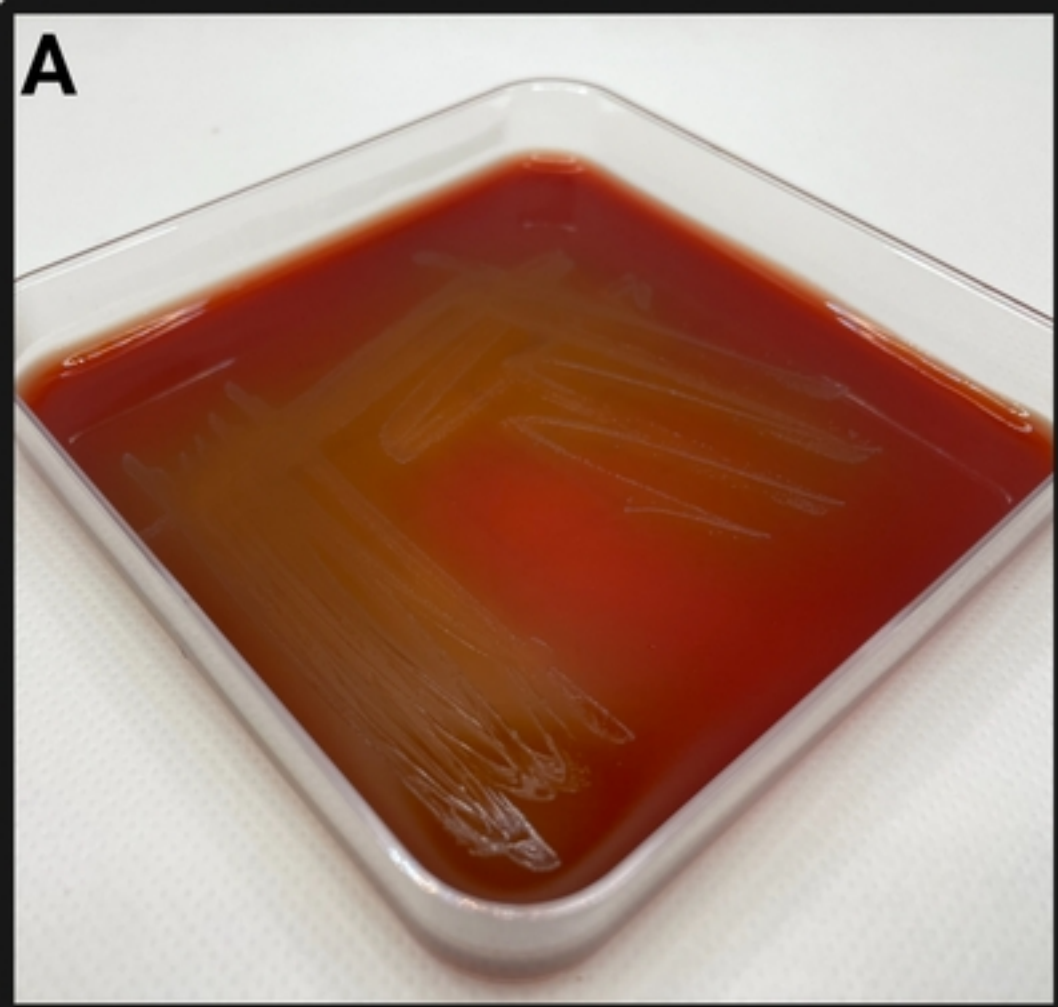
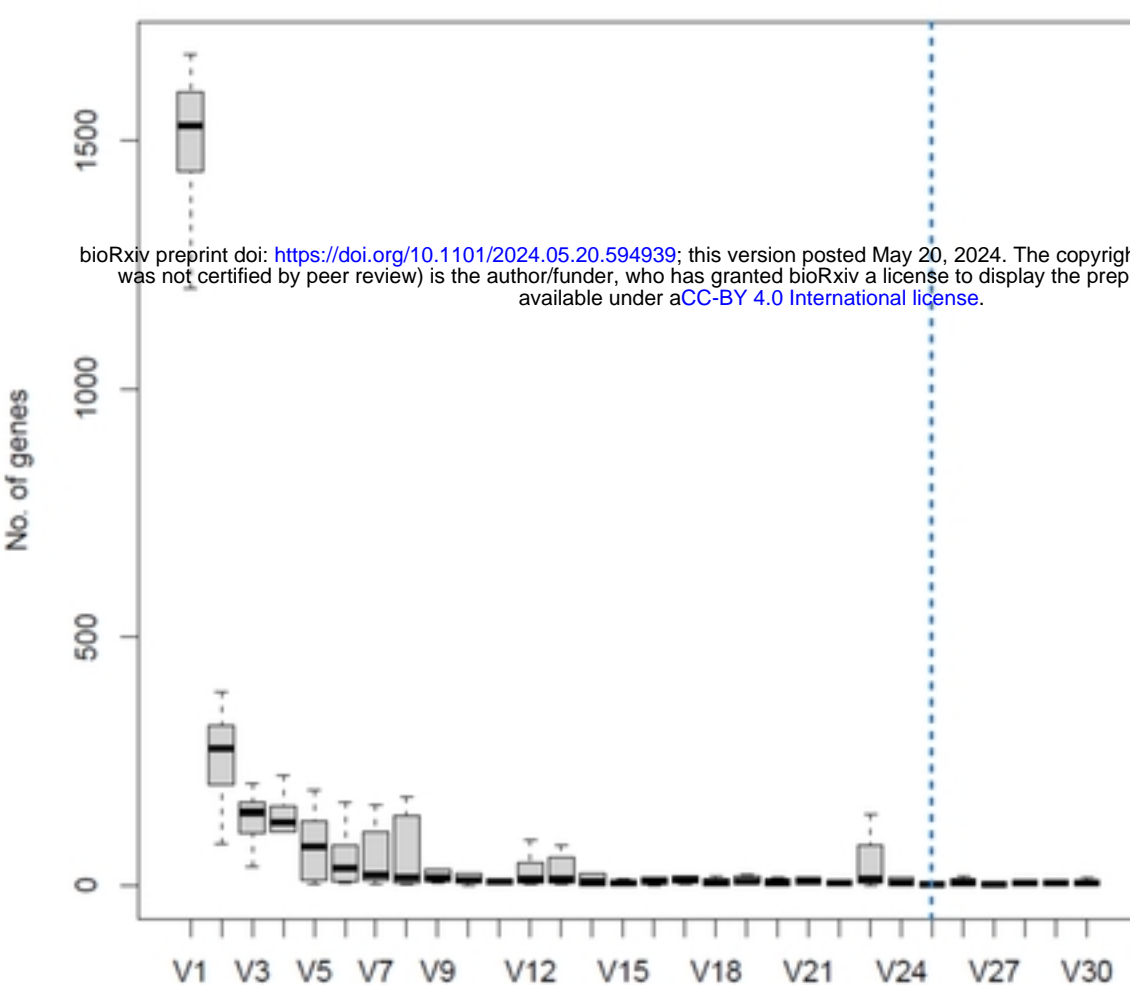
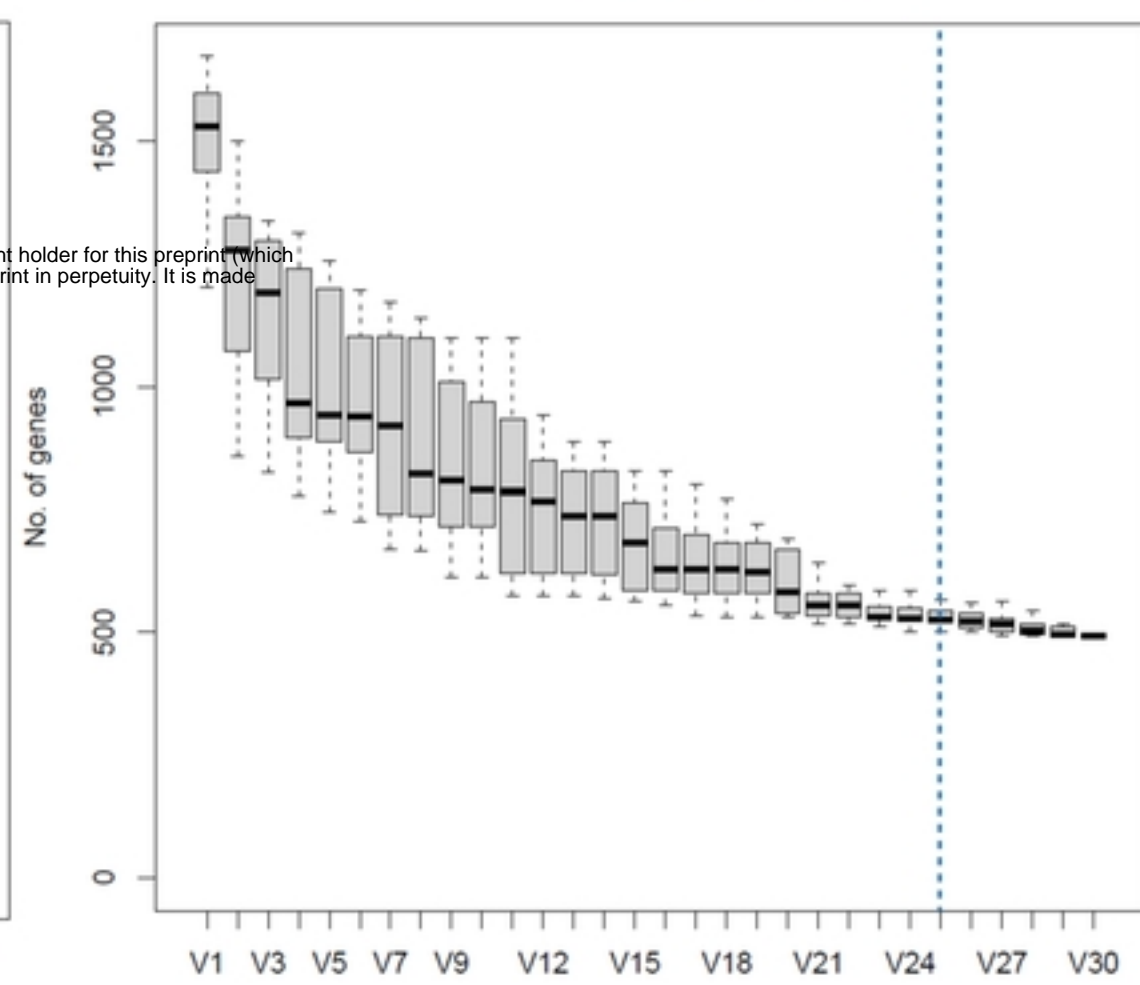
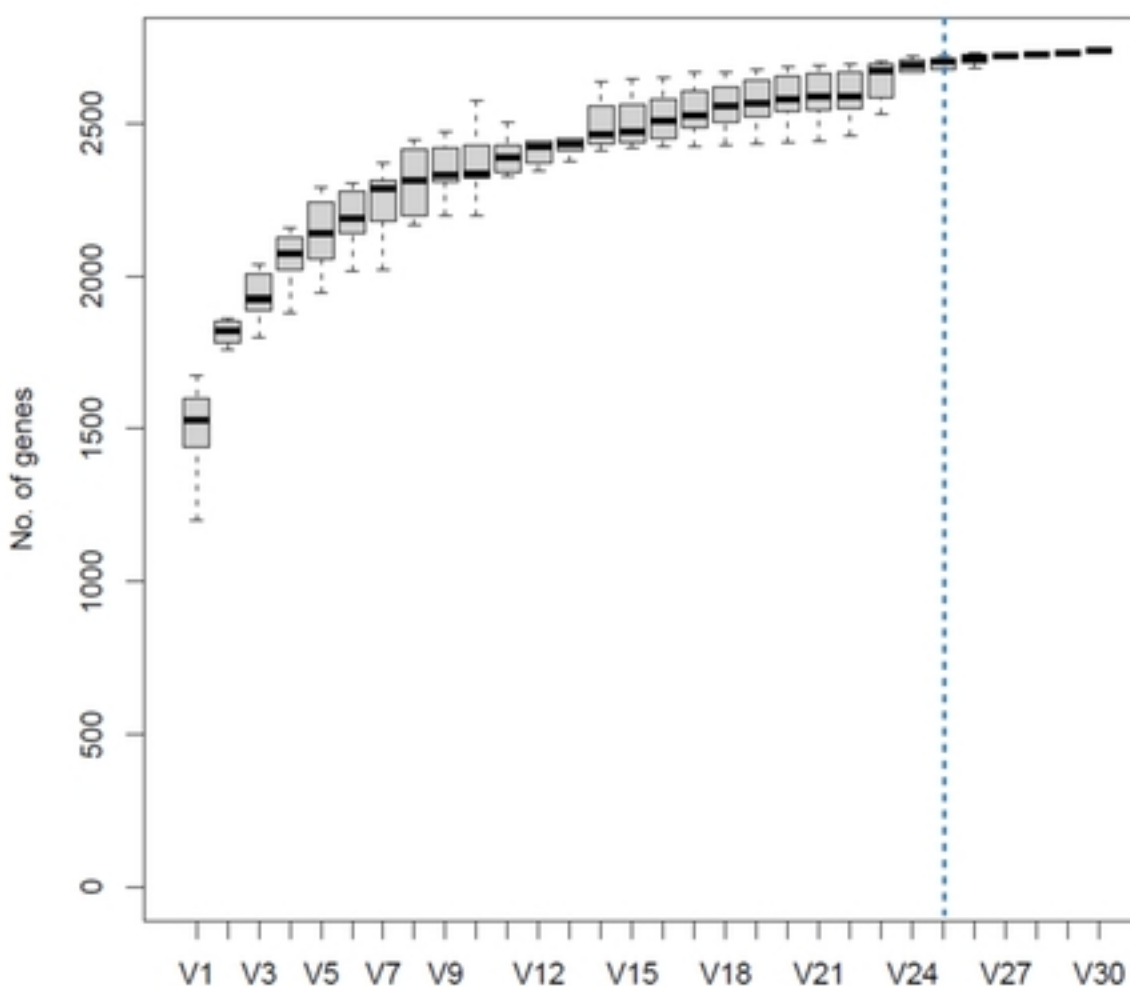
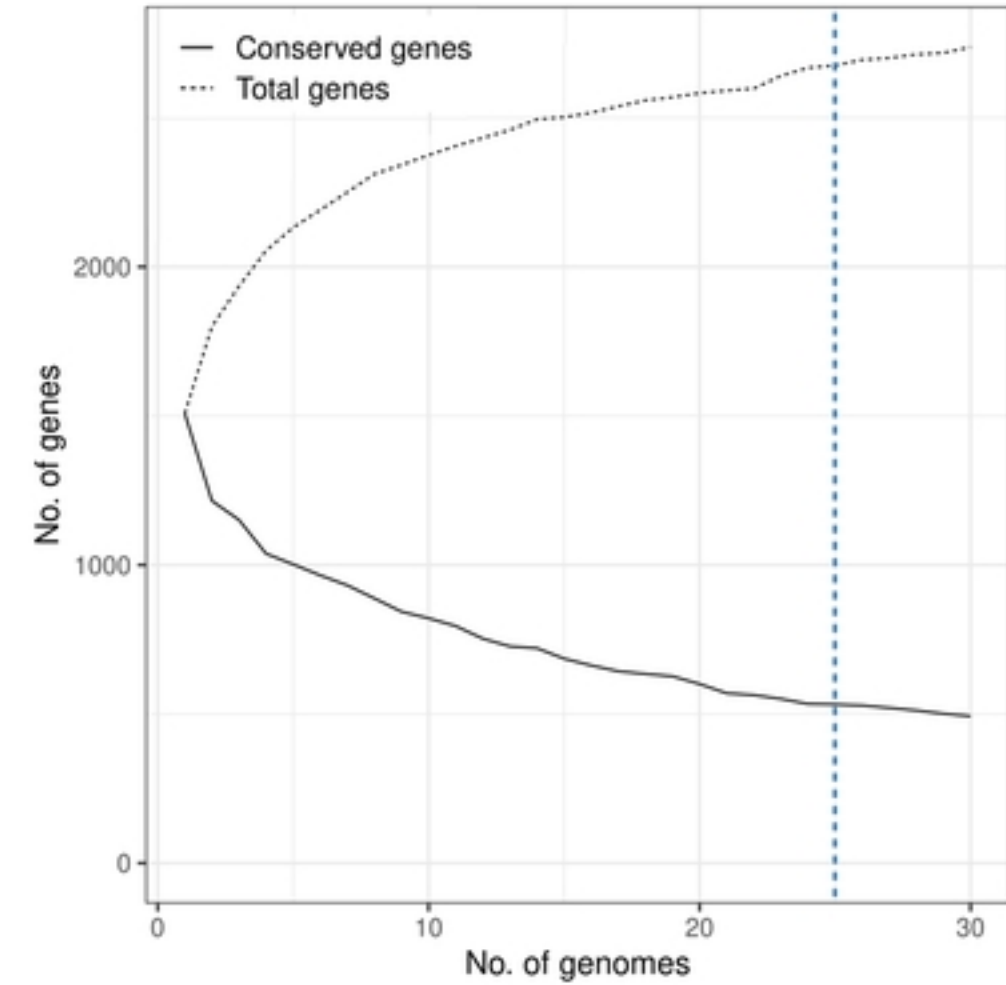
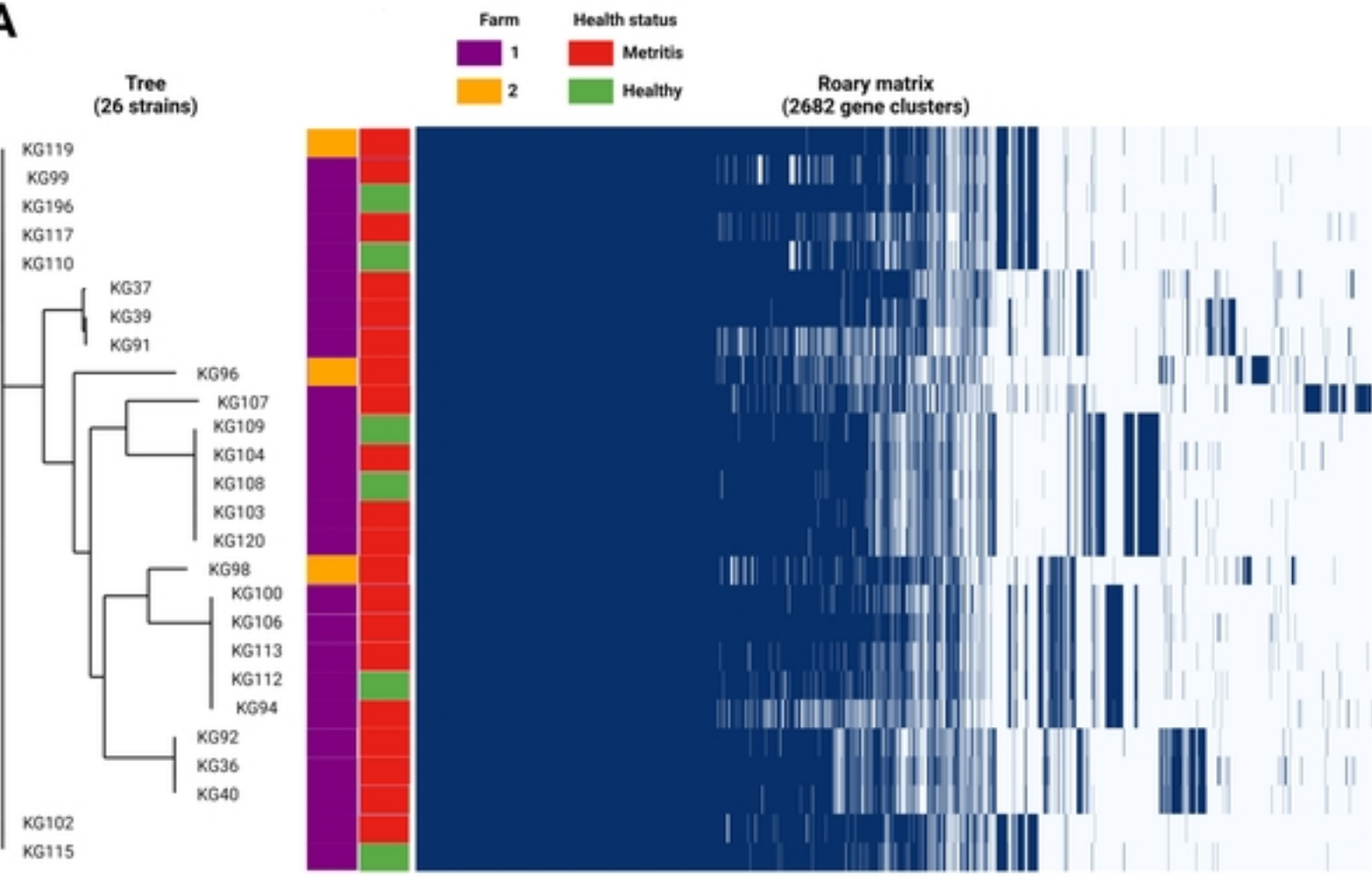
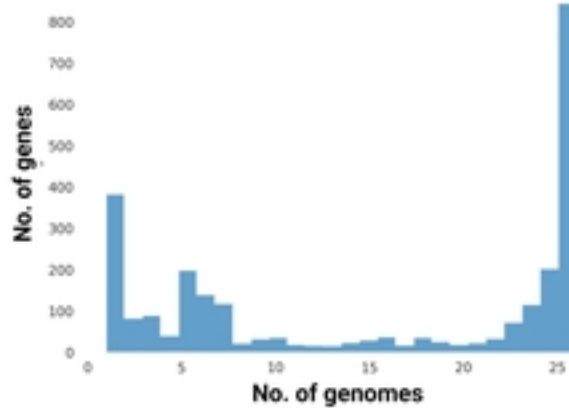
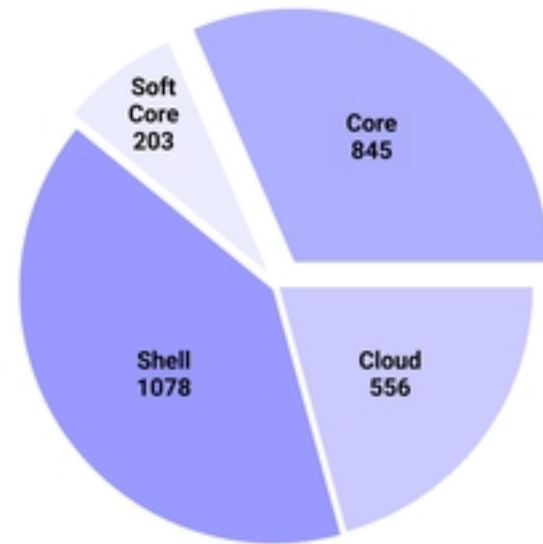


Figure 5

A**Number of new genes****B****Number of conserved genes****C****No. of genes in the pan-genome****D****Figure 6**

A**B****C****Figure 7**

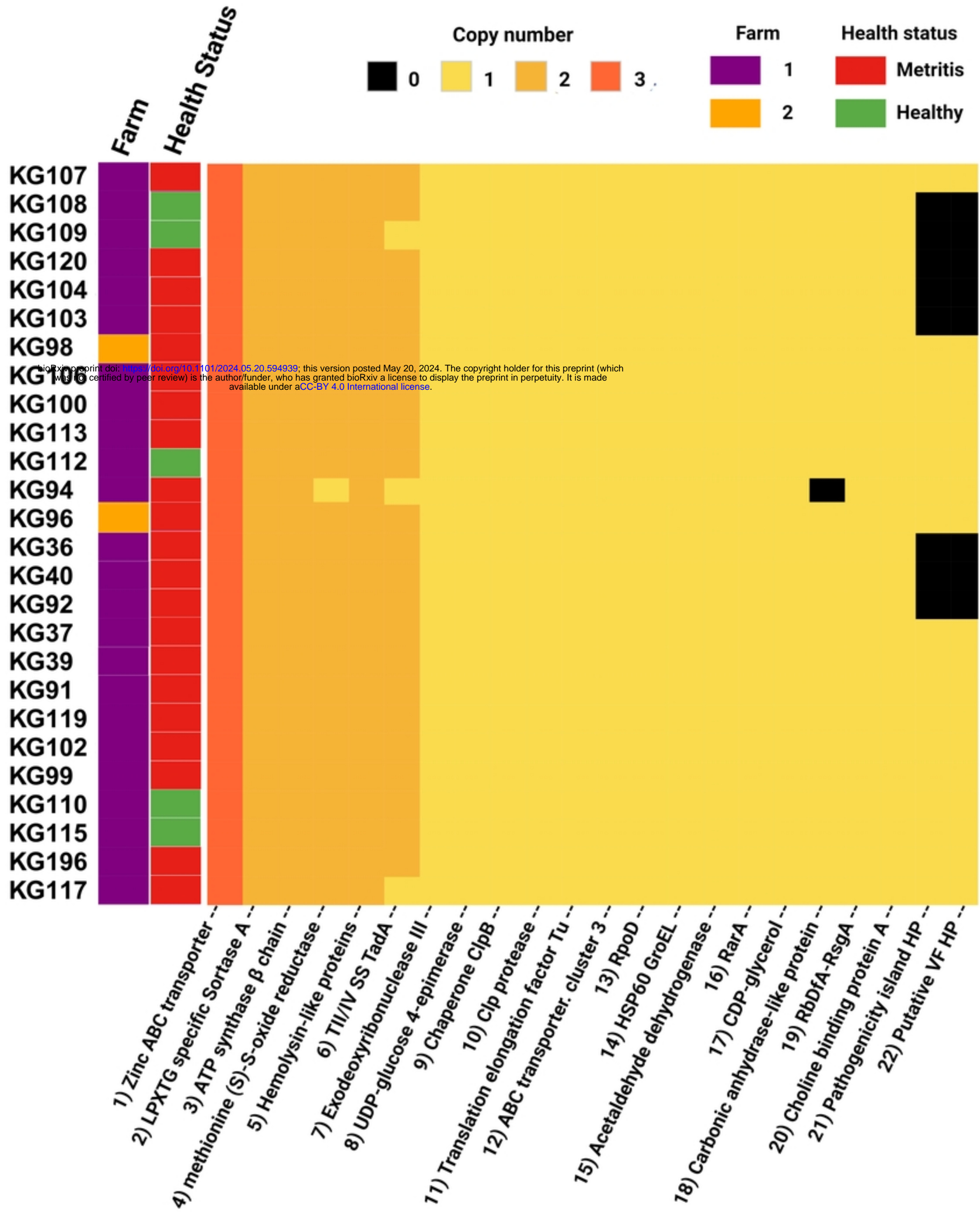


Figure 8

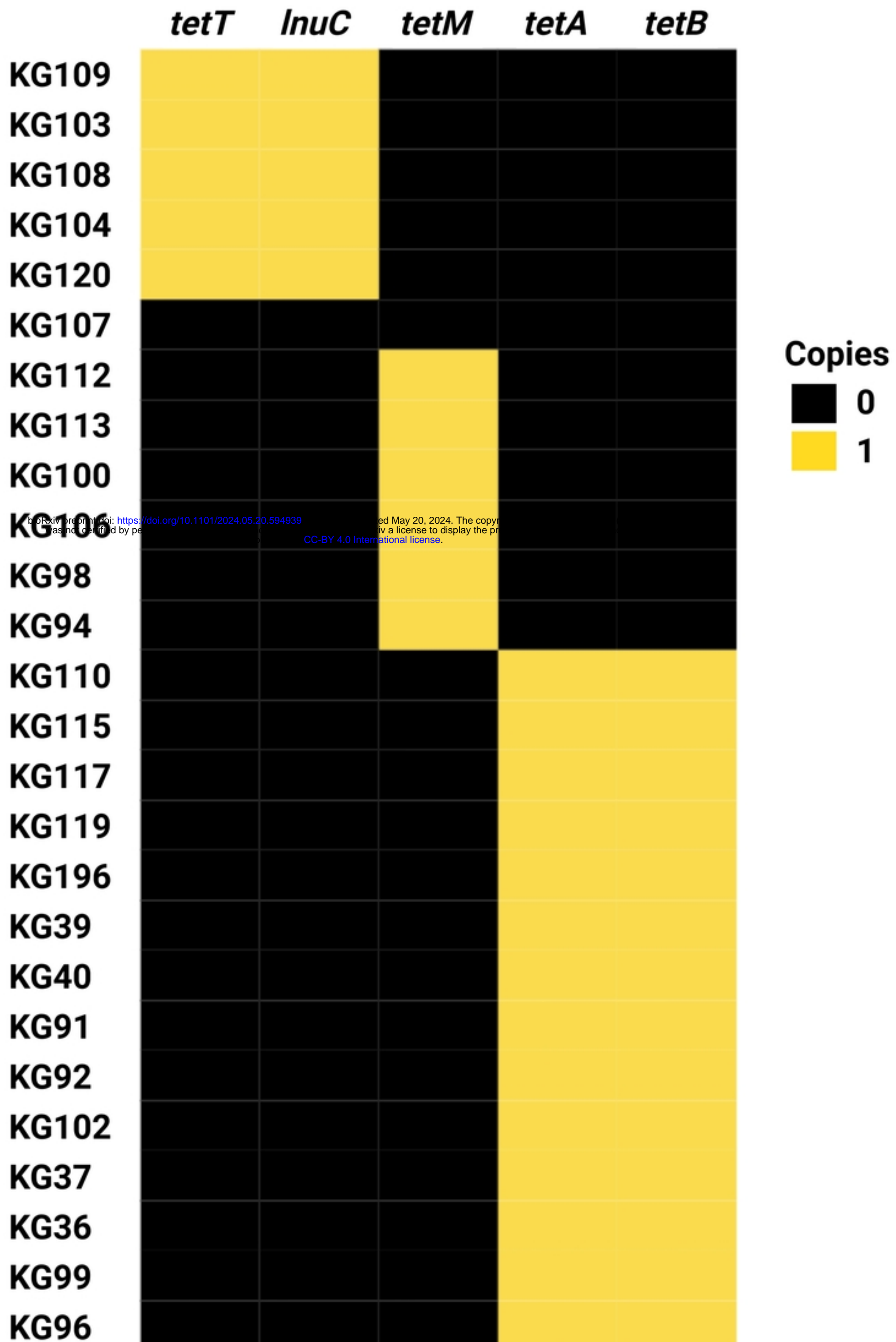


Figure 9